NASA Technical Memorandum 100596

COUPLED BENDING-TORSION STEADY-STATE RESPONSE OF PRETWISTED, NONUNIFORM ROTATING BEAMS USING A TRANSFER-MATRIX METHOD

Carl E. Gray, Jr.

March 1988

National Aeronautics and
Space Administration

Langley Research Center
Hampton, Virginia 23665-5225

ABSTRACT

COUPLED BENDING-TORSION STEADY-STATE RESPONSE OF PRETWISTED, NONUNIFORM ROTATING BEAMS USING A TRANSFER-MATRIX METHOD

Using the Newtonian method, the equations of motion are developed for the coupled bending-torsion steady-state response of beams rotating at constant angular velocity in a fixed plane. The resulting equations are valid to first order strain-displacement relationships for a long beam with all other nonlinear terms retained. In addition, the equations are valid for beams with the mass centroidal axis offset (eccentric) from the elastic axis, nonuniform mass and section properties, and variable twist. The solution of these coupled, nonlinear, nonhomogeneous, differential equations is obtained by modifying a Hunter linear second-order transfer-matrix solution procedure to solve the nonlinear differential equations and programing the solution for a desk top personal computer. The modified transfer-matrix method was verified by comparing the solution for a rotating beam with a geometric, nonlinear, finite-element computer code solution; and for a simple rotating beam problem, the modified method demonstrated a significant advantage over the finite-element solution in accuracy, ease of solution, and actual computer processing time required to effect a solution.

TABLE OF CONTENTS

	Page
LIST OF TABLES	v
LIST OF FIGURES	vi
LIST OF SYMBOLS	ix
Chapter	
1. INTRODUCTION	1
2. MATHEMATICAL FORMULATION	5
2.1 Analysis of Displacement	5
2.2 Analysis of Strain	9
2.3 Analysis of Inertial Loads	12
2.4 Development of Governing Equations	16
2.4.1 Derivation of Equilibrium Condition	16
2.4.2 Internal Elastic Loads	18
3. FORMULATION OF GOVERNING EQUATIONS AS A CLASSICAL BOUNDARY VALUE PROBLEM	23
3.1 Differential Equations	23
3.2 Boundary Conditions	26
4. TRANSFER-MATRIX SOLUTION METHOD	29
4.1 Fourth-order Runge-Kutta Transfer Matrix	30
4.2 Fourth-order Transfer-Matrix Error Estimate	33
5. COMPUTER PROGRAMS	34
5.1 Program PROP - Calculate fan blade cross-sectional properties	34
5.2 Program SOLVE - Transfer-matrix solution of nonhomogeneous nonlinear, boundary-value problems	35

TABLE OF CONTENTS (CONTINUED)

		Page
6.	RESULTS OF APPLICATION	37
	6.1 Nonuniform, Noneccentric, Twisted, Fan Blade	37
	6.1.1 Transfer-Matrix Solution	37
	6.1.2 Nonlinear Finite-Element Solution	39
	6.1.3 Transfer-Matrix and Finite-Element Solution Comparison	39
	6.2 Nonuniform, Eccentric, Twisted, Fan Blade	41
	6.2.1 Fully Coupled Transfer-Matrix Solution	42
	6.2.2 Partially Coupled Transfer-Matrix Solution	42
	6.2.3 Fully Coupled and Partially Coupled Transfer-Matrix Solution Comparison	43
7.	CONCLUDING REMARKS	45
REFERENCES		47
APPENDICES		
A	THEORETICAL DERIVATION OF THE HUNTER TRANSFER-MATRIX METHOD	48
B	CALCULATION OF 7- BY 10-FOOT WIND TUNNEL FAN BLADE SECTION PROPERTIES	54

LIST OF TABLES

Table		Page
6.1	Aerodynamic Design Load Intensities	38
6.2	Support Reaction Comparison	41

LIST OF FIGURES

Figure		Page
2.1	Geometry and sign convention of rotating beam	60
2.2	Cross-sectional geometry	60
2.3	Cross-sectional deformations	61
2.4	Orientation of rotating beam in undeformed configuration	62
2.5	Rotating beam under steady-state aerodynamic loads	62
2.6	Equilibrium of differential bending element	63
2.7	Internal elastic loads	64
2.8	Contribution of longitudinal stress to the internal elastic torque	65
3.1	Governing differential equations in matrix format	66
5.1	Flow chart of program PROP	67
5.2	Flow chart of program SOLVE	68
6.1	Comparison of axial displacements	69
6.2	Comparison of beamwise displacement	69
6.3	Comparison of chordwise displacements	70
6.4	Comparison of cross-sectional twist	70
6.5	Comparison of Θ_y rotations	71
6.6	Comparison of Θ_z rotations	71
6.7	Axial displacement	72
6.8	Beamwise transverse bending displacement	72
6.9	Chordwise transverse bending displacement	73

LIST OF FIGURES (CONTINUED)

Figure		Page
6.10	Beam twist, ϕ	73
6.11	Bending rotation, Θ_y	74
6.12	Bending rotation, Θ_z	74
6.13	Axial force, T	75
6.14	Beamwise shear force, V_y	75
6.15	Chordwise shear force, V_z	76
6.16	Twisting moment, M_x	76
6.17	Beam bending moment, M_y	77
6.18	Beam bending moment, M_z	77
B.1	Typical airfoil cross-sectional geometry	78
B.2	7- by 10-Foot Wind Tunnel fan blade	78
B.3	7- by 10-Foot Wind Tunnel fan blade station 57.375	79
B.4	7- by 10-Foot Wind Tunnel fan blade station 60.000	79
B.5	7- by 10-Foot Wind Tunnel fan blade station 66.000	80
B.6	7- by 10-Foot Wind Tunnel fan blade station 74.000	80
B.7	7- by 10-Foot Wind Tunnel fan blade station 78.000	81
B.8	7- by 10-Foot Wind Tunnel fan blade station 82.000	81
B.9	7- by 10-Foot Wind Tunnel fan blade station 84.000	82
B.10	7- by 10-Foot Wind Tunnel fan blade station 96.000	82
B.11	7- by 10-Foot Wind Tunnel fan blade station 106.000	83
B.12	7- by 10-Foot Wind Tunnel fan blade station 116.000	83
B.13	7- by 10-Foot Wind Tunnel fan blade station 126.000	84
B.14	7- by 10-Foot Wind Tunnel fan blade station 136.000	84
B.15	7- by 10-Foot Wind Tunnel fan blade station 146.000	85

LIST OF FIGURES (CONCLUDED)

Figures		Page
B.16	7- by 10-Foot Wind Tunnel fan blade station 156.000 . . .	85
B.17	7- by 10-Foot Wind Tunnel fan blade station 166.000 . . .	86
B.18	7- by 10-Foot Wind Tunnel fan blade station 173.000 . . .	86

SYMBOLS

c	chord length of airfoil cross section
ds, ds_1	element lengths of fiber before and after straining
e	numerical integration error estimate
h	increment of variable x
i, j, k	unit vectors
o	origin of y-z axes
$\underline{r}$	position vector to arbitrary undeformed cross-sectional point
$\underline{r}_m$	position vector to center of mass
$\underline{r}_1$	position vector to arbitrary deformed cross-sectional point
x, y, z	Cartesian coordinates
x_m, y_m, z_m	coordinates of the center of mass
x_1, y_1, z_1	components of $\underline{r}_1$
$\bar{y}_1$, $\bar{z}_1$	coordinate of center of mass in y_1-z_1 system
u, v, w	elastic displacements of elastic axis
A	cross-sectional area
A_x, A_y	centrifugal acceleration components of the center of mass
C_ϕ	nonlinear coefficient
E	modulus of elasticity
G	shear modulus
GJ	St. Venant torsional stiffness

SYMBOLS (CONTINUED)

J	torsional stiffness constant
I_{yy}, I_{zz}, I_{yz}, I_p	moments of inertia about y-z blade reference axes
$I_{y_1y_1}$, $I_{z_1z_1}$, $I_{y_1z_1}$	moments of inertia about y_1-z_1 axes
M_x, M_y, M_z	moments
T	tension due to centrifugal force
P	location of point on cross section
P_1, P_2, P_3, P_4, P_5	area cross-section integrals about y-z system
$\overline{P}_1$, $\overline{P}_2$, $\overline{P}_3$, $\overline{P}_4$, $\overline{P}_5$	area cross-section integrals about y_1-z_1 system
P_y, P_z, q_x	aerodynamic loads resolved to elastic axis
V_y, V_z	shear forces
$\overline{X}_m$, $\overline{Y}_m$, $\overline{Z}_m$	coordinates of center of mass as defined in equations (2.27), (2.28), (2.29)
β	pretwist blade angle of cross section
β_t	transformation angle between y_1-z_1 and y-z system
δ	arbitrary constant
ε	longitudinal strain
η, ζ	beam reference coordinate system
Ω	angular velocity of blade about its axis of rotation
ρ	mass density of blade
σ	longitudinal normal stress
ϕ, θ_y, θ_z	rotations of a cross section of a blade
ψ, λ	blade geometry cross-section reference system
ψ_s, λ_s	coordinates of the shear center
ψ_u, ψ_ℓ, λ_u, λ_ℓ	coordinates of the upper and lower surface of blade cross section

SYMBOLS (CONCLUDED)

Matrices

$[A]$	state matrix (coefficients of differential equations)
$[\overline{A}]$	average of [A] matrices at the i and i+1 stations
$\{B\}$	transfer vector
$\{\overline{B}\}$	average of {B} vectors at the i and i+1 stations
$\{b_1\}$, $\{b_2\}$, $\{b_3\}$, $\{b_4\}$	Runge-Kutta integrating vectors
$[\overline{C}]$	coefficient matrix equation (3.13)
$[C]$, $[D]$	boundary matrices
$[E]$, $[G]$	transfer matrices
$\{F\}$, $\{H\}$	transfer vectors
$[I]$	identity matrix
$\{P\}$, $\{Q\}$	boundary vectors
$\{Y\}$	field vector

CHAPTER 1

INTRODUCTION

At the Langley Research Center there are several wind tunnels which are driven by rotating propeller or fan blade systems. Nearly all of these tunnels have been in operation for several years; and in order to ensure safe and continued operation, the existing blades will require a thorough evaluation of the steady-state response under the current operating conditions. To determine the steady-state response of rotating blades, effective and efficient analysis techniques are required that consider the unique features common to rotating systems.

An important consideration in the structural analysis of a rotating beam is the effect of the coupling between the centrifugal force and the elastic stiffness (deflections) of the beam. This effect provides a stiffer structural member in both the beamwise and chordwise directions. To solve this problem and take advantage of the centrifugal-stiffening effect is difficult due to the necessity of having to know the deformed state of the beam in order to apply the steady-state centrifugal loads.

The literature is extensive with current and classical papers concentrating on the rotating beam problem. Among the more notable is

the linear analyses of Houbolt and Brooks [1]*. In their paper, they systematically develop the governing differential equations for the coupled bending and torsion of pretwisted blades assuming shear and rotary inertia are negligible. The warping rigidity for a slender beam was implicitly considered by incorporating a St. Venant torsion term in the internal elastic torque equation. Hunter [2] developed a system of linear coupled differential equations for small displacements where the axial displacement and centrifugal force equations easily uncouple, and allows the axial component equations to be solved separately from the transverse component equations. These equations illustrate the basic but essential physics of the rotating beam and were developed specifically to demonstrate an integrating-matrix method for solving homogeneous differential equations. Shear and rotatory inertia effect were considered by Stafford and Giurgiutiu [3] for the uncoupled uniform vibrating beam rotating in a fixed plane. They found that these effects were more noticeable for blades operating at higher speeds (turbomachinery blades). These and other similar papers, however, center around predicting the natural vibration characteristics [2,3,4] of rotor blades (rotating beams). The concern with the natural vibration problem is to accurately determine mode shapes and natural frequencies of rotors to avoid resonance. The natural vibration problem, in effect, solves the eigenvalue problem resulting from eliminating the nonhomogeneous part of the governing equations of motion. Solutions of the eigenvalue problem are important in the design of rotating beams, but solutions for the

---

* The numbers in brackets indicate reference.

steady-state response of the rotating beam are also important for determining strength for fatigue evaluation and distortions for clearance evaluations.

The purpose of this thesis is to address the development and solution of the governing equations of pretwisted rotating beams under the influence of steady-state aerodynamic and inertial loadings (the nonlinear nonhomogeneous boundary-value problem) using a transfer-matrix method. The transfer-matrix solution method has been selected because of its capability to account for the variation of the beam's geometry (stiffness and mass) and loading along the span of the beam.

Chapter 2 first develops the kinematics of the longitudinal deformations of the beam including uniform extension, bending about two axes, and uniform twist. Second, the stress resultants for a linear elastic material are developed using the longitudinal strain. Following the development of the internal stress resultants, the acceleration of a differential element where the elastic and centroidal axes are not coincident is derived for a steady-state rotating element. By application of D'Alembert's principle to the resulting steady-state inertial loads, the equilibrium equations for a differential element under transverse and torque loadings are developed. Chapter 3 formulates the resulting 12, coupled, nonlinear, first-order, ordinary differential equations derived in Chapter 2 into a classical boundary-value problem. Since the intended application of this development is to provide a complete analytical tool, Chapter 4 presents a nonlinear solution method for solving the derived equations, and Chapter 5 discusses the computer programs necessary to

implement the solution algorithm. Chapter 6 describes an application of the theory, solution algorithm, and computer programs necessary to analyze a new fan blade design for the 7- by 10-Foot Wind Tunnel at the Langley Research Center. Results from the transfer-matrix approach are evaluated by comparison with finite-element results. In Appendix A, a derivation of the second-order Hunter transfer-matrix method is presented, and Appendix B gives the details of calculating the necessary cross-sectional integrals for a typical 7- by 10-Foot Wind Tunnel fan blade.

CHAPTER 2

MATHEMATICAL FORMULATION

The system of displacements for a generalized flexure theory is derived based upon the assumption that regardless of the loading, the original shape of the cross section is unaltered during deformations. Thus, the geometric dimensions of every plane normal to the longitudinal axis of the beam remains unchanged. Note, however, that this assumption precludes any type of out-of-plane cross-sectional deformations (neglect warping and shear deformations). Following from these displacements, the longitudinal strains are developed as is done by Houbolt and Brooks [1] for a beam under both lateral, extensional, and twisting motion. After expressing the inertial loads on a beam in terms of the deformations, the derivation then considers the equilibrium of a deformed beam in terms of its geometry and resultant loads, thus, yielding a set of nonlinear governing differential equations for the longitudinal, transverse, and torsional deformations of an elastic structure.

2.1 Analysis of Displacements

The cross-sectional plane defined by x equals a constant (see figure 2.1) is allowed to undergo u, v, and w displacements of the elastic axis. In addition, the cross section is allowed to rotate Θ_y

and Θ_z about the y and z coordinate axes, respectively. The cross-sectional twist, ϕ, is measured about the elastic axis, x. By passing a plane through the beam that is normal to the cross-section's x-axis, the location of a point, P, on the pretwisted cross-section may be described for both the undeformed (figure 2.2(a)) and deformed, (figure 2.2(b)) beam. Attached to the cross-section is a (η,ζ) coordinate system that moves with the deforming cross-section and is located at the shear center. The angle β locates the positive η-axis which locates the principal minor axis of inertia relative to the positive y-axis.

The position vector $\underline{r}$ to the point P in the y-z and η-ζ coordinate systems is given by

$$\underline{r} = \begin{Bmatrix} x \\ \eta \\ \zeta \end{Bmatrix} = \begin{bmatrix} 1 & 0 & 0 \\ 0 & \cos(\beta) & \sin(\beta) \\ 0 & -\sin(\beta) & \cos(\beta) \end{bmatrix} \begin{Bmatrix} x \\ y \\ z \end{Bmatrix} \tag{2.1}$$

$$\underline{r} = \begin{Bmatrix} x \\ y \\ z \end{Bmatrix} = \begin{bmatrix} 1 & 0 & 0 \\ 0 & \cos(\beta) & -\sin(\beta) \\ 0 & \sin(\beta) & \cos(\beta) \end{bmatrix} \begin{Bmatrix} x \\ \eta \\ \zeta \end{Bmatrix} \tag{2.2}$$

The rate of change, using primes to denote differentiation with respect to x, of the point P with respect to the longitudinal axis is then given by

$$\begin{Bmatrix} y' \\ z' \end{Bmatrix} = \beta' \begin{bmatrix} -\sin(\beta) & -\cos(\beta) \\ \cos(\beta) & -\sin(\beta) \end{bmatrix} \begin{Bmatrix} \eta \\ \zeta \end{Bmatrix} \tag{2.3}$$

Using equation (2.1) in (2.3) yields

$$\begin{Bmatrix} y' \\ z' \end{Bmatrix} = \beta' \begin{Bmatrix} -z \\ y \end{Bmatrix} \tag{2.4}$$

Next by imposing the u, v, and w displacements at the elastic axis and also rotating the cross section by the angle ϕ, the position vector $\underline{r_1}$ (see figure 2.2) is expressed in terms of the original position vector $\underline{r}$ and the cross-sectional displacements. Recall that the fundamental assumption of this development is that the original cross-section does not change its shape: this implies that the vector $\underline{r}$ relative to the η-ζ system is unaffected. Thus, only the kinematics of the cross section in the y-z system are evaluated.

The x_1 component of the $\underline{r_1}$ vector is composed of contributions due to extension and bending about the y and z axes. Therefore, by superimposing the extension (figure 2.3(a)) and bending (figures 2.3(b) and 2.3(c)) effects, the x_1 component is

$$x_1 = x + u - y \frac{dv}{dx} - z \frac{dw}{dx} \tag{2.5}$$

or by using primes to denote differentiation with respect to x,

$$x_1 = x + u - y\, v' - z\, w' \tag{2.5}$$

The other two components of $\underline{r_1}$, y_1 and z_1, are found by using equation (2.2) with the pretwist angle, β, replaced by the total twist, $(\beta+\phi)$.

$$\begin{Bmatrix} y_1 \\ z_1 \end{Bmatrix} = \begin{bmatrix} \cos(\beta + \phi) & -\sin(\beta + \phi) \\ \sin(\beta + \phi) & \cos(\beta + \phi) \end{bmatrix} \begin{Bmatrix} \eta \\ \zeta \end{Bmatrix} \tag{2.6}$$

In addition, if the usual small-angle assumptions are made for ϕ and using double-angle trigonometric identities, then equation (2.6) becomes

$$\begin{Bmatrix} y_1 \\ z_1 \end{Bmatrix} = \begin{bmatrix} [\cos(\beta) - \phi \sin(\beta)] & [-\sin(\beta) + \phi \cos(\beta)] \\ [\sin(\beta) + \phi \cos(\beta)] & [\cos(\beta) - \phi \sin(\beta)] \end{bmatrix} \begin{Bmatrix} \eta \\ \zeta \end{Bmatrix} \tag{2.7}$$

Expanding equation (2.7) and using equation (2.1) leads to

$$\begin{Bmatrix} y_1 \\ z_1 \end{Bmatrix} = \begin{Bmatrix} y \\ z \end{Bmatrix} + \phi \begin{Bmatrix} -z \\ y \end{Bmatrix} \tag{2.8}$$

Superimposing the v and w displacements of the elastic axis and including equation (2.5), the position vector $\underline{r}_1$ becomes

$$\bar{r}_1 = \begin{Bmatrix} x_1 \\ y_1 \\ z_1 \end{Bmatrix} = \begin{Bmatrix} x + u - y\, v' - z\, w' \\ v + y - z\, \phi \\ w + z + y\, \phi \end{Bmatrix} \tag{2.9}$$

Using equation (2.9), the rate of change of $\underline{r}_1$ with respect to x is given by

$$\underline{r}_1' = \begin{Bmatrix} x_1' \\ y_1' \\ z_1' \end{Bmatrix} = \begin{Bmatrix} 1 + u' - y'\, v' - y\, v'' - z'\, w' - z\, w'' \\ v' + y' - z'\, \phi - z\, \phi' \\ w' + z' + y'\, \phi + y\, \phi' \end{Bmatrix} \tag{2.10}$$

Collecting terms and using equation (2.4), equation (2.10) becomes

$$\underline{r_1}' = \begin{Bmatrix} x_1' \\ y_1' \\ z_1' \end{Bmatrix} = \begin{Bmatrix} 1 + u' - y(v'' + \beta' w') - z(w'' - \beta' v') \\ v' - y \beta' \phi - z(\beta' + \phi') \\ w' + y(\beta' + \phi') - z \beta' \phi \end{Bmatrix} \quad (2.11)$$

Thus, after deformation, the position vector of a point, P, is given by equation (2.9), and its derivative with respect to x is given by equation (2.11).

2.2 Analysis of Strain

From the displacement analysis results, the longitudinal strain, ε, that is developed in a longitudinal fiber, is derived analytically. Let the point P under displacements (u,v,w) of point o (elastic axis, see figure 2.2(b)) and rotations (ϕ, v', w') of the cross-section, be displaced to P' (x_1, y_1, z_1) on the rotated cross-sectional plane as given by equation (2.9). Then the differential length, ds_1, correponds to

$$(ds_1)^2 = (dx_1)^2 + (dy_1)^2 + (dz_1)^2 \quad (2.12)$$

or

$$(ds_1')^2 = (x_1')^2 + (y_1')^2 + (z_1')^2 \quad (2.13)$$

Performing the indicated algebra and using equation (2.11), each of the components on the right hand side of equation (2.13) has the following form

$$(x_1')^2 = 1 + 2u' + (u')^2$$
$$+ (- 2v''- 2w'\beta'- 2u'v''- 2\beta'u'w')y$$
$$+ (- 2w''+ 2v'\beta' - 2u'w''+ 2 \beta'u'v')z$$
$$+ (2v''w'' - 2\beta'v'v'' - 2(\beta')^2v'w' + 2\beta'w') yz$$
$$+ ((v'')^2 + 2\beta'w'v'' + (\beta')^2(w')^2)y^2$$
$$+ ((w'')^2 - 2\beta'v'w'' + (\beta')^2(v')^2)z^2 \qquad (2.14)$$

$$(y_1')^2 = (v')^2 + (-2 \beta'v'\phi)y + (-2 \beta'v' - 2 \phi'v') z$$
$$+ (2(\beta')^2\phi + 2 \beta'\phi'\phi)yz + ((\beta')^2(\phi)^2) y^2$$
$$+ ((\beta')^2 + 2 \beta'\phi' + (\phi')^2)z^2 \qquad (2.15)$$

$$(z_1')^2 = (w')^2 + (2\beta'w' + 2w'\phi')y + (- 2 \beta'w'\phi)z$$
$$+ (-2(\beta')^2\phi - 2 \beta'\phi'\phi)yz + ((\beta')^2 + 2\beta'\phi' + (\phi')^2)y^2$$
$$+ ((\beta')^2(\phi)^2)z^2 \qquad (2.16)$$

Substituting equations (2.14)-(2.16) into equation (2.13) leads to

$$(s_1')^2 = \underline{1} + \underline{2u'} + (u')^2 + (v')^2 + (w')^2$$
$$+(\underline{-2v''} - 2u'v'' - 2u'w'\beta' - 2 \beta'v'\phi + 2\phi'w')y$$
$$+(\underline{-2w''} - 2u'w'' + 2u'v'\beta' - 2 \beta'w'\phi - 2\phi'v')z$$
$$+(2v''w'' - 2v'\beta'v'' + 2w'\beta'w'' - 2v'w'(\beta')^2)yz$$
$$+((v'')^2 + 2w'\beta'v'' + (w')^2(\beta')^2 + \underline{(\beta')^2} + \underline{2\beta'\phi'}$$
$$+ (\phi')^2 + (\beta')^2(\phi)^2)y^2$$
$$+((w'')^2 - 2v'\beta'w'' + (v')^2(\beta')^2 + \underline{(\beta')^2} + \underline{2\beta'\phi'}$$
$$+ (\phi')^2 + (\beta')^2(\phi)^2)z^2$$

(2.17)

For this development, the assumption is that the problem formulation be restricted to small displacements. Thus, the second-order terms in equation (2.17) are much less than unity; therefore, only the first-order displacement terms, (underlined in equation 2.17), are retained.

$$\frac{ds_1}{dx} = \left[1 + 2u' - 2yv'' - 2zw'' + (y^2 + z^2)((\beta')^2 + 2\beta'\phi')\right]^{1/2} \tag{2.18}$$

Taking the initial length of ds to correspond to $u = v = w = \phi = 0$, equation (2.18) reduces to

$$\frac{ds}{dx} = \left[1 + (y^2 + z^2)(\beta')^2\right]^{1/2} \tag{2.19}$$

Making use of the fundamental definition of longitudinal strain to the first order in dx

$$\varepsilon = \frac{ds_1 - ds}{ds} \tag{2.20}$$

and equations (2.18) and (2.19), the following result is obtained

$$\varepsilon = \frac{\{1 + 2u' - 2yv'' - 2zw'' + (y^2 + z^2)(\beta'^2 + 2\beta'\phi)\}^{.5} - \{1 + (y^2 + z^2)\beta'^2\}^{.5}}{\left(1 + (y^2 + z^2)(\beta')^2\right)^{.5}} \tag{2.21}$$

Noting that each of the square root terms in equation (2.11) is of the form

$$(1 + \delta)^{1/2} \tag{2.22}$$

which can be, for small δ, approximated by

$$1 + \delta/2 \tag{2.23}$$

Making use of equation (2.23), then equation (2.21) can be reduced to

$$\varepsilon = \frac{u' - yv'' - zw'' + (y^2 + z^2)\beta'\phi'}{1 + (y^2 + z^2)\frac{(\beta')^2}{2}} \tag{2.24}$$

A closer evaluation of the second term in the denominator of equation (2.24), for most rotating beams that are used as fan blades and propellers, reveals that the $(\beta')^2$ term is usually on the order of 1° per inch. This can, for most geometries, reduce the second term to the order of 0.01 which is much less than unity; therefore, it is neglected. This yields the final linear expression for the longitudinal strain of

$$\varepsilon = u' - yv'' - zw'' + (y^2 + z^2)\beta'\phi' \tag{2.25}$$

As pointed out in reference [1], the above expression for the longitudinal strain includes the effects of four general types of motion: uniform longitudinal extension of the cross section; rotation of the cross section due to two axes bending; and rotation of cross-sectional planes relative to each other about the elastic axis due to twisting of the beam.

2.3 Analysis of Inertial Loads

The acceleration of a rotating beam is determined at the centroid of the segment, see figure 2.4. For this derivation, the axis of

rotation is assumed to coincide with the z-axis, which is normal to the elastic axis. Thus, the location of the center of mass on the cross section is given by

$$\underline{r}_m = \bar{X}_m \underline{i} + \bar{Y}_m \underline{j} + \bar{Z}_m \underline{k} \tag{2.26}$$

where the components of $\underline{r}_m$, in the deformed configuration, are determined by using equation (2.9).

$$\bar{X}_m = x_m + u - y_m v' - z_m w' \tag{2.27}$$

$$\bar{Y}_m = y_m + v - z_m \phi \tag{2.28}$$

$$\bar{Z}_m = z_m + w + y_m \phi \tag{2.29}$$

The origin of the elastic axis is assumed to coincide with an inertial frame such that the elastic-axis coordinate system is seen as just a rotating system with respect to this inertial frame. Thus, the position vector, equation (2.26), describes the location of the center of mass of each cross-section explicitly in terms of the undeformed location and the displacement components; therefore, the time derivatives (denoted by dots) of the position vector are easily determined. The velocity of the center of mass is given by

$$\dot{\underline{r}}_m = \dot{\bar{X}}_m \underline{i} + \bar{X}_m \dot{\underline{i}} + \dot{\bar{Y}}_m \underline{j} + \bar{Y}_m \dot{\underline{j}} + \dot{\bar{Z}}_m \underline{k} + \bar{Z}_m \dot{\underline{k}} \tag{2.30}$$

Since the $\underline{i}$, $\underline{j}$, and $\underline{k}$ system is just rotating with respect to the inertial frame, the time derivatives of the bases vectors are

$$\dot{\underline{i}} = \Omega \quad \underline{j} \tag{2.31}$$

$$\dot{\underline{j}} = -\Omega \quad \underline{i} \tag{2.32}$$

$$\dot{\underline{k}} = 0. \tag{2.33}$$

Also, the time derivatives of the components of the position vector $\underline{r}_m$ are

$$\dot{\bar{X}}_m = \dot{u} - y_m \dot{v}' - z_m \dot{w}' \tag{2.34}$$

$$\dot{\bar{Y}}_m = \dot{v} - z_m \dot{\phi} \tag{2.35}$$

$$\dot{\bar{Z}}_m = \dot{w} + y_m \dot{\phi} \tag{2.36}$$

Using equations (2.31)-(2.33), equation (2.30) becomes

$$\dot{\underline{r}}_m = (\dot{\bar{X}}_m - \Omega \bar{Y}_m)\,\underline{i} + (\dot{\bar{Y}}_m + \Omega \bar{X}_m)\,\underline{j} + \dot{\bar{Z}}_m \underline{k} \tag{2.37}$$

Following the same approach, the acceleration of the center of mass of a cross section, assuming a constant rotation, is

$$\ddot{\underline{r}}_m = (\ddot{\bar{X}}_m - 2\Omega \dot{\bar{Y}}_m - \Omega^2 \bar{X}_m)\underline{i} + (\ddot{\bar{Y}}_m + 2\Omega \dot{\bar{X}}_m - \Omega^2 \bar{Y}_m)\underline{j} + \ddot{\bar{Z}}_m \underline{k} \tag{2.38}$$

where

$$\ddot{\bar{X}}_m = \ddot{u} - y_m \ddot{v}' - z_m \ddot{w}' \tag{2.39}$$

$$\ddot{\bar{Y}} = \ddot{v} - z_m \ddot{\phi} \tag{2.40}$$

$$\ddot{\bar{Z}}_m = \ddot{w} + y_m \ddot{\phi} \tag{2.41}$$

Upon substituting equations (2.39)-(2.41) into equation (2.38), the acceleration of the center of mass becomes

$$\begin{aligned} \ddot{\underline{r}}_m = & [\ddot{u} - y_m\ddot{v}' - z_m\ddot{w}' - 2\,\Omega(\dot{v} - z_m\dot{\phi}) - \Omega^2(x_m+u-y_m v' - z_m w')]\,\underline{i} \\ & [\ddot{v} - z_m\ddot{\phi} + 2\,\Omega(\dot{u} - y_m\dot{v}' - z_m\dot{w}') - \Omega^2(y_m + v - z_m\phi)\,]\,\underline{j} \\ & [\,\ddot{w} + y_m\ddot{\phi}\,]\,\underline{k} \end{aligned} \tag{2.42}$$

For the purpose of this analysis, the motion of concern is the steady-state response of the beam. Thus, all time derivatives are zero; and equation (2.42) becomes

$$\begin{aligned} \ddot{\underline{r}}_m &= -\Omega^2\,(x_m + u - y_m\,v' - z_m\,w')\,\underline{i} - \Omega^2(y_m + v - z_m\,\phi)\,\underline{j} \\ &= A_x\,\underline{i} + A_y\,\underline{j} \end{aligned} \tag{2.43}$$

2.4 Development of Governing Equation

2.4.1 Derivation of Equilibrium Condition

For the derivation of the equilibrium conditions of a rotating beam as shown in figure 2.5, attention is restricted to the steady-state response of a beam that is rotating at a constant angular velocity under steady-state aerodynamic lift (P_z), drag (P_y), and torque (q_x). The aerodynamic loads are assumed to be resolved to the elastic axis as varying distributive loads.

A differential beam segment is shown in figure 2.6 with its associated loads: internal, inertial, and aerodynamic. For the steady response of a rotating beam, the differential inertial loads are assumed to act at the center of mass of the differential segment. Using D'Alembert's principle of dynamic equilibrium, the inertial loads are treated as if they were applied static forces, but in the opposite sense. Referring to figure 2.6(a), the axial equilibrium condition is

$$T + \frac{dT}{dx} dx - T - \rho A_x dx = 0 \tag{2.44}$$

Upon substituting the $\underline{i}$-component of equation (2.43) into equation (2.44) and simplifying, the governing equation for the tension becomes

$$\frac{dT}{dx} + \rho \Omega^2 (x_m + u - y_m v' - z_m w') = 0 \tag{2.45}$$

Summing the forces in the y-direction, figure 2.6(b), the following equilibrium equation is derived

$$V_y + \frac{dV_y}{dx} dx - \rho A_y dx - V_y + P_y dx = 0 \qquad (2.46)$$

Using equation (2.43), equation (2.46) becomes

$$\frac{dV_y}{dx} + \rho \Omega^2 (v + y_m - z_m \phi) + P_y = 0 \qquad (2.47)$$

Similarly, the z-force equilibrium equation is derived, see figure 2.6(c).

$$V_z + \frac{dV_z}{dx} dx - V_z + P_z dx = 0 \qquad (2.48)$$

or

$$\frac{dV_z}{dx} + P_z = 0 \qquad (2.49)$$

The sum of the moments in the x-y plane, about the center of the differential element, figure 2.6(b), yields the following

$$M_z + \frac{dM_z}{dx} dx - M_z - \rho A_x (y_m - z_m \phi) dx + \frac{dx}{2} (V_y + \frac{dV_y}{dx} dx) + \frac{dx}{2} V_y$$

$$-v' \frac{dx}{2} (T + \frac{dT}{dx} dx) - v' \frac{dx}{2} T = 0 \qquad (2.50)$$

Dividing through by dx, using equation (2.43) for A_x, and taking the limit as dx goes to zero, equation (2.50) reduces to

$$\frac{dM_z}{dx} - \rho\,\Omega^2(x_m\,y_m + u\,y_m - v'y_m^2 - w'z_m\,y_m - x_m\,z_m\,\phi - u\,z_m\phi$$

$$+ v'y_m\,z_m\,\phi + w'z_m^2\phi) + V_y - v'T = 0 \qquad (2.51)$$

Similarly the moment equilibrium equation in the x-z plane is derived

$$\frac{dM_y}{dx} + \rho\,\Omega^2(x_m\,z_m + u\,z_m - v'y_m\,z_m - w'z_m^2 + x_m\,y_m\,\phi + u\,y_m\phi$$

$$-v'y_m^2\,\phi - w'y_m\,z_m\phi) - V_z + w'T = 0 \qquad (2.52)$$

From figure 2.6(a), the equilibrium equation for the y-z plane (torque) is

$$\frac{dM_x}{dx} + q_x - \rho\,\Omega^2\,(z_m\,v + y_m\,z_m - z_m^2\,\phi + y_m\,v\,\phi + y_m^2\,\phi - z_m\,y_m\,\phi^2) = 0 \qquad (2.53)$$

There are now 6 equations, (2.45,47,49,51-53), and 10 unknowns (T, V_y, V_z, M_x, M_y, M_z, u, v, w, ϕ) which indicates that additional relationships are required. The additional equations can be developed from the internal elastic equilibrium (stress resultant) constraint imposed on a cross section that the integrated stresses balance the resultant loads at the elastic axis.

2.4.2 Internal Elastic Loads

By assuming the longitudinal material orientation of the rotating beam behaves as a linear elastic material, the constituent relationship can be described by Hooke's law.

$$\sigma = E\,\varepsilon \qquad (2.54)$$

where E is the apparent longitudinal modulus of elasticity, and ε is given in equation (2.25).

From the above definition, the stress distribution over the cross-section may be resolved into the internal resisting loads at the elastic axis, see figure 2.7.

The axial, T, and bending, M_y and M_z, internal loads are given by

$$T = \int \sigma \, dA \tag{2.55}$$

$$M_y = \int \sigma \; z \, dA \tag{2.56}$$

$$M_z = -\int \sigma \; y \, dA \tag{2.57}$$

By introducing the minus sign on the M_z component, a tensile longitudinal stress will be produced when a negative M_z is introduced; this makes the sign of the normal stress consistent with the sense of the internal load, see figure 2.6a. As pointed out by Houbolt and Brooks[1], the selection of the elastic axis as the primary reference axis was to eliminate the shearing stresses that are associated with the longitudinal stresses from contributing to the total resisting torque, M_x. Because of the pretwist, the longitudinal stress has a component that contributes to the internal torque (see figure (2.8)). From figure (2.8), it is seen that the inplane components of the normal stress produce a torque

$$M_{xn} = \int \sigma \, (\eta^2 + \zeta^2) \, (\beta' + \phi') \, dA \tag{2.58}$$

Substituting equation (2.1) into equation (2.58) and noting that the Jocobian relating the differential areas in the y-z and η-ζ systems is unity, equation (2.58) becomes

$$M_{xn} = \int \sigma \, (\beta' + \phi')[\, y^2 + z^2 \,]dA \tag{2.59}$$

As is done in [1], equation (2.59) is combined with the St. Venant twisting which leads to the following equation for the total resisting internal torque.

$$M_x = \int \sigma \, (\beta' + \phi')[\, y^2 + z^2 \,]dA \; + GJ\phi' \tag{2.60}$$

For convenience, the internal resisting loads are restated again using equation (2.25)

$$T = E \int (u' - yv'' - zw'' + (y^2 + z^2)\beta'\phi')dA \tag{2.61}$$

$$M_y = E \int z(u' - yv'' - zw'' + (y^2 + z^2)\beta'\phi')dA \tag{2.62}$$

$$M_z = -E \int y(u' - yv'' - zw'' + (y^2+z^2)\beta'\phi')dA \tag{2.63}$$

$$M_x = E \int (y^2 + z^2)(\beta' + \phi')(u' - yv'' - zw'' + (y^2 + z^2)\beta'\phi')dA + GJ\phi' \tag{2.64}$$

By making use of the following definitions,

$$A = \int dA \qquad \text{(typical units in}^2\text{)} \tag{2.65}$$

$$I_{yy} = \int z^2\, dA \qquad \text{(typical units in}^4\text{)} \tag{2.66}$$

$$I_{zz} = \int y^2\, dA \qquad \text{(typical units in}^4\text{)} \tag{2.67}$$

$$I_{yz} = \int yz\, dA \qquad \text{(typical units in}^4\text{)} \tag{2.68}$$

$$I_p = \int (y^2 + z^2)\, dA \qquad \text{(typical units in}^4\text{)} \tag{2.69}$$

$$P_1 = \int y\, dA \qquad \text{(typical units in}^3\text{)} \tag{2.70}$$

$$P_2 = \int z\, dA \qquad \text{(typical units in}^3\text{)} \tag{2.71}$$

$$P_3 = \int z(y^2 + z^2)\, dA \qquad \text{(typical units in}^5\text{)} \tag{2.72}$$

$$P_4 = \int y(y^2 + z^2)\, dA \quad \text{(typical units in}^5\text{)} \tag{2.73}$$

$$P_5 = \int (y^2 + z^2)^2\, dA \quad \text{(typical units in}^6\text{)} \tag{2.74}$$

the integrations, as indicated, in equations (2.61)-(2.64) can be performed to yield the following

$$T = E\,[\, A\,u' - P_1\,v'' - P_2\,w'' + I_p\,\beta'\,\phi'\,] \tag{2.75}$$

$$M_y = E\,[\, P_2\,u' - I_{yz}\,v'' - I_{yy}\,w'' + P_3\,\beta'\,\phi'\,] \tag{2.76}$$

$$M_z = E\,[-P_1\,u' + I_{zz}\,v'' + I_{yz}\,w'' - P_4\,\beta'\,\phi'\,] \tag{2.77}$$

$$M_x = GJ\,\phi' + E\,[\, I_p\,\beta'u' - P_4\,\beta'\,v'' - P_3\,\beta'\,w'' + P_5\,(\beta')^2\,\phi' + I_p\,\phi'u' - P_4\,\phi'\,v'' - P_3\,\phi'\,w'' + P_5\,(\phi')^2] \tag{2.78}$$

Equations (2.75)-(2.78) define the internal elastic equilibrium which relates the internal forces to displacements. This now increases the number of equations to 10, and thus, ensures a compatible system of equations and unknowns.

CHAPTER 3

FORMULATION OF GOVERNING EQUATIONS AS A CLASSICAL BOUNDARY-VALUE PROBLEM

The preceding analysis has furnished a set of coupled nonlinear differential equations. These equations together with constraints or conditions on the boundaries comprise the classical boundary-value problem. This chapter is an organized summary of the previously derived governing equations recast and formatted in a form that yields a system of first-order differential equations.

3.1 Differential Equations

To summarize, the six equilibrium equations (2.45), (2.47), (2.48), (2.51), (2.52), and (2.53) are restated.

$$\frac{dT}{dx} = - \rho \Omega^2 (x_m + u - y_m v' - z_m w') \tag{3.1}$$

$$\frac{dV_y}{dx} = - \rho \Omega^2 (v + y_m - z_m \phi) - P_y \tag{3.2}$$

$$\frac{dV_z}{dx} = - P_z \tag{3.3}$$

$$\frac{dM_x}{dx} = -q_x + \rho \Omega^2 (z_m v + y_m z_m - z_m^2 \phi + y_m v \phi + y_m^2 \phi - z_m y_m \phi^2) \tag{3.4}$$

$$\frac{dM_y}{dx} = -\rho\,\Omega^2(x_m z_m + u z_m - v'y_m z_m - w'z_m^2 + x_m y_m \phi + uy_m \phi$$

$$- v'y_m^2 \phi - w'y_m z_m \phi) + V_z - w'T \qquad (3.5)$$

$$\frac{dM_z}{dx} = \rho\,\Omega^2(x_m y_m + u y_m - v'y_m^2 - w'z_m y_m - x_m z_m \phi - u z_m \phi$$

$$+ v'y_m z_m \phi + w'z_m^2 \phi) - V_y + v'T \qquad (3.6)$$

Similarly, the stress resultant equilibrium equations (2.75-78) are restated.

$$T = E [A u' - P_1 v'' - P_2 w'' + I_p \beta' \phi'] \qquad (3.7)$$

$$M_y = E [P_2 u' - I_{yz} v'' - I_{yy} w'' + P_3 \beta' \phi'] \qquad (3.8)$$

$$M_z = E [-P_1 u' + I_{zz} v'' + I_{yz} w'' - P_4 \beta' \phi'] \qquad (3.9)$$

$$M_x = GJ \phi' + E [I_p \beta' u' - P_4 \beta' v'' - P_3 \beta' w'' + P_5 (\beta')^2 \phi'$$

$$+ I_p \phi' u' - P_4 \phi' v'' - P_3 \phi' w'' + P_5 (\phi')^2] \qquad (3.10)$$

Since the proposed solution method utilizes matrix methods, equations (3.7-10) are written as first order differential equations in matrix form by letting

$$\begin{Bmatrix} v' \\ w' \end{Bmatrix} = \begin{bmatrix} 0 & 1 \\ -1 & 0 \end{bmatrix} \begin{Bmatrix} \Theta_y \\ \Theta_z \end{Bmatrix} \qquad (3.11)$$

$$\begin{bmatrix} EA & E\,\beta' I_p & E\,P_2 & -E\,P_1 \\ E\,\beta' I_p & GJ + C\phi & E\beta'\,P_3 & -E\,\beta'\,P_4 \\ E\,P_2 & E\,\beta'\,P_3 & E\,I_{yy} & -E\,I_{yz} \\ -E\,P_1 & -E\,\beta'\,P_4 & -E\,I_{yz} & E\,I_{zz} \end{bmatrix} \begin{Bmatrix} u' \\ \phi' \\ \Theta_y' \\ \Theta_z' \end{Bmatrix} = \begin{Bmatrix} T \\ M_x \\ M_y \\ M_z \end{Bmatrix} \tag{3.12}$$

where $C\phi = E\,I_p\,u' - E\,P_4\,\Theta_z' + E\,P_3\,\Theta_y' + E\,P_5\,\phi' + E\,P_5\,(\beta')^2$

Equation (3.12) is of the form

$$\left[\bar{C}\right] \begin{Bmatrix} u' \\ \phi' \\ \Theta_y' \\ \Theta_z' \end{Bmatrix} = \begin{Bmatrix} T \\ M_x \\ M_y \\ M_z \end{Bmatrix} \tag{3.13}$$

Since equation (3.12) is nonsingular, the solution of (3.12) or (3.13) can be obtained.

$$\begin{Bmatrix} u' \\ \phi' \\ \Theta_y' \\ \Theta_z' \end{Bmatrix} = \left[\bar{C}\right]^{-1} \begin{Bmatrix} T \\ M_x \\ M_y \\ M_z \end{Bmatrix} \tag{3.14}$$

Figure 3.1 is a summary of the twelve first order differential equations in matrix form. These 12 equations are now in a form that is easily integrated by a transfer-matrix method. The general character of the equations is that four of the equations result in solutions for the unknown displacement (u, v, w, ϕ), and six of the equations yield solutions for the generalized loads while the remaining two equations (3.11) are definitions to reduce the second order differential equations (3.7-10) to first-order differential equations.

3.2 Boundary Conditions

As is the case with most boundary-value problems, the types of boundary conditions that can be specified are generally either geometric, natural, or a complicated combination of both. One special feature of the transfer-matrix solution method is that it can easily handle any combination of homogeneous or nonhomogeneous, natural or geometric boundary conditions. For the rotating beam, the boundary conditions are geometric at the fixed support end and natural at the free or cantilevered end.

In terms of the coordinate system shown in figure 2.7, the boundary conditions for complete fixity (constrained against all displacements) at the support are

$$u = v = w = \phi = \Theta_y = \Theta_z = 0 \qquad (3.15)$$

For a free end (free to displace) the boundary conditions are

$$T = V_y = V_z = M_x = M_y = M_z = 0 \qquad (3.16)$$

If there were, for example, a tip mass attached to the rotating beam, the axial force as well as the shear forces at the free end may be nonzero which results in nonhomogeneous conditions. Again, this apparent complication, as is shown in the applications sections, is no more difficult to handle than the homogeneous conditions.

The above boundary conditions can also be represented in a matrix format.

Fixed end (geometric) -

$$\begin{bmatrix} 1 & 0 & 0 & 0 & 0 & 0 & 0 & 0 & 0 & 0 & 0 & 0 \\ 0 & 1 & 0 & 0 & 0 & 0 & 0 & 0 & 0 & 0 & 0 & 0 \\ 0 & 0 & 1 & 0 & 0 & 0 & 0 & 0 & 0 & 0 & 0 & 0 \\ 0 & 0 & 0 & 1 & 0 & 0 & 0 & 0 & 0 & 0 & 0 & 0 \\ 0 & 0 & 0 & 0 & 1 & 0 & 0 & 0 & 0 & 0 & 0 & 0 \\ 0 & 0 & 0 & 0 & 0 & 1 & 0 & 0 & 0 & 0 & 0 & 0 \end{bmatrix} \begin{Bmatrix} u \\ v \\ w \\ \phi \\ \Theta_y \\ \Theta_z \\ T \\ V_y \\ V_z \\ M_x \\ M_y \\ M_z \end{Bmatrix} = [0] \qquad (3.17)$$

Free end (natural) -

$$\begin{bmatrix} 0&0&0&0&0&0&1&0&0&0&0&0 \\ 0&0&0&0&0&0&0&1&0&0&0&0 \\ 0&0&0&0&0&0&0&0&1&0&0&0 \\ 0&0&0&0&0&0&0&0&0&1&0&0 \\ 0&0&0&0&0&0&0&0&0&0&1&0 \\ 0&0&0&0&0&0&0&0&0&0&0&1 \end{bmatrix} \begin{Bmatrix} u \\ v \\ w \\ \phi \\ \Theta_y \\ \Theta_z \\ T \\ V_y \\ V_z \\ M_x \\ M_y \\ M_z \end{Bmatrix} = [0] \qquad (3.18)$$

CHAPTER 4

TRANSFER-MATRIX SOLUTION METHOD

A method is developed for numerically computing the solution of a set of coupled, first-order, nonhomogeneous, nonlinear differential equations. The solution technique employs an integration similar to the Hunter method[1] which is extended here to a fourth-order Runge-Kutta scheme to improve the numerical accuracy when limited station properties are available.

The technique of using the transfer matrix to solve a wide class of boundary-value problems can readily be found in the literature. However, the earlier development of the transfer matrix was primarily employed to solve the homogeneous problem [5,6]. This approach proved to be a useful analytical tool in determining the natural modes and frequencies of vibrating beams, wings, and propellers. Other matrix methods such as the integrating-matrix [2] have also been employed, with a great deal of success, to solve the nonhomogeneous problem. More recent application of the transfer-matrix method [7], addresses

---

[1] The Hunter method, which was developed in 1974, is an undocumented transfer-matrix solution process that can easily account for the nonhomogeneous part of a set of first-order differential equation. A complete development of the method is presented in appendix A.

both the nonhomogeneous and the homogeneous boundary-value problem. These methods, however, require an extensive library of transfer and point matrices as well as some manipulation of the matrices to satisfy and impose boundary conditions. In addition, each new class of boundary-value problems requires a special technique to derive the transfer-matrix from the differential equations. In the present paper, the presented method allows for a more direct solution of the boundary-value problem by formulating the transfer matrix directly from the differential equations and solving the linear equations completely in two passes over the solution domain. The first pass is required to satisfy all boundary conditions, both natural and geometric; and the second pass computes the solution at the selected stations within the closed interval defined by the boundary points.

4.1 Fourth-order Runge-Kutta Transfer Matrix

The Hunter transfer-matrix (appendix A) method can be shown to parallel a second-order Runge-Kutta integration. Using this fact, an improvement on the accuracy of the Hunter method is easily obtained by directly applying a fourth-order Runge-Kutta to equation (A.1).

$$\{Y'\} = [A]\ \{Y\} + \{B\} \tag{4.1}$$

Rewriting equation (4.1) in the following functional form

$$\{Y'\} = F\ (x,\ Y) \tag{4.2}$$

and using a standard fourth-order Runge-Kutta integration [8], the value of {Y} at the (i+1) station in terms of the value of {Y} at the i station is

$$\{Y_{i+1}\} = \{Y_i\} + 1/6\ (\{b_1\} + 2\ \{b_2\} + 2\ \{b_3\} + \{b_4\}) \tag{4.3}$$

where the {b}'s are defined to be

$$\{b_1\} = h_i\ F(x_i,\ \{Y_i\}) \tag{4.4}$$

$$\{b_2\} = h_i\ F(x_i + 1/2\ h_i,\ \{Y_i\} + 1/2\ \{b_1\}) \tag{4.5}$$

$$\{b_3\} = h_i\ F(x_i + 1/2\ h_i,\ \{Y_i\} + 1/2\ \{b_2\}) \tag{4.6}$$

$$\{b_4\} = h_i\ F(x_i + h_i,\ \{Y_i\} + \{b_3\}) \tag{4.7}$$

Using equation (4.2) in equations (4.4-7) yields

$$\{b_1\} = h_i\ [A_i]\ \{Y_i\} + h_i\ \{B_i\} \tag{4.8}$$

$$\{b_2\} = hi\ [\overline{A}]\ \{Y_i\} + \frac{h_i^2}{2}\ [\overline{A}]\ [A_i]\ \{Y_i\} + h_i\ \{\overline{B}\} + \frac{h_i^2}{2}\ [\overline{A}]\ \{B_i\} \tag{4.9}$$

$$\{b_3\} = h_i\ [A_i]\ \{Y_i\} + \frac{h_i^2}{2}\ [A]\ [\overline{A}]\ \{\overline{Y}_i\} + \frac{h_i^3}{4}\ [A]\ [\overline{A}]\ [\overline{A}_i]\ \{Y_i\} + h_i\ \{\overline{B}\} + \frac{h_i^2}{2}\ [\overline{A}]\ \{\overline{B}\} + \frac{h_i^3}{4}\ [\overline{A}]\ [\overline{A}]\ \{B_i\} \tag{4.10}$$

$$\{b_4\} = h_i\ [A_{i+1}]\ \{Y_i\} + h_i^2\ [A_{i+1}]\ [\overline{A}]\ \{Y_i\} + \frac{h_i^3}{2}\ [A_{i+1}]\ [\overline{A}]\ [\overline{A}]\ \{Y_i\} + \frac{h_i^4}{4}\ [A_{i+1}]\ [\overline{A}]\ [\overline{A}]\ [A_i]\ \{Y_i\} + h_i\ \{B_{i+1}\} + h_i^2\ [A_{i+1}]\ \{\overline{B}\} + \frac{h_i^3}{2}\ [A_{i+1}]\ [\overline{A}]\ \{\overline{B}\} + \frac{h_i^4}{4}\ [A_{i+1}]\ [A]\ [\overline{A}]\ \{\overline{B}_i\} \tag{4.11}$$

where the $[\overline{A}]$ and $\{\overline{B}\}$ matrices are the average of the [A] and {B} matrices at the i th and i+1 station, respectively.

Substituting equations (4.8-11) into equation (4.3), collecting terms, and developing an equation similar to equation (A.10), new [E] and {F} transfer matrices like those in equations (A.11) and (A.12) can be defined as follows

$$[E_i] = [I] + \frac{h_i}{6}([A_i] + 4[\overline{A}] + [A_{i+1}])$$

$$+ \frac{h_i^2}{6}([\overline{A}]\,[A_i] + [\overline{A}]\,[\overline{A}] + [A_{i+1}]\,[\overline{A}])$$

$$+ \frac{h_i^3}{12}([\overline{A}]\,[\overline{A}]\,[A_i] + [A_{i+1}]\,[\overline{A}]\,[\overline{A}])$$

$$+ \frac{h_i^4}{24}[A_{i+1}]\,[\overline{A}]\,[\overline{A}]\,[A_i] \qquad (4.12)$$

$$\{F_i\} = \frac{h_i}{6}(\{B_i\} + 4\,\{\overline{B}\} + \{B_{i+1}\})$$

$$+ \frac{h_i^2}{6}([\overline{A}]\,\{B_i\} + [\overline{A}]\,\{\overline{B}\} + [A_{i+1}]\,\{\overline{B}\})$$

$$+ \frac{h_i^3}{12}([\overline{A}]\,[\overline{A}]\,\{B_i\} + [A_{i+1}]\,[\overline{A}]\,\{\overline{B}\})$$

$$+ \frac{h_i^4}{24}[A_{i+1}]\,[\overline{A}]\,[\overline{A}]\,\{B_i\} \qquad (4.13)$$

From these new definitions of the transfer matrices (4.12) and (4.13), the rest of the solution, equations (A.13-17), can be directly applied as usual.

In addition to solving linear problems, the Hunter method, using either a second-order or a fourth-order Runge-Kutta integration, can be used to solve nonlinear differential equations. This is accomplished simply by collecting the nonlinear terms in the [A] matrix (or the {B} vector) and iterating the solution until successive {Y} values differ by no more than some predetermined (convergence criteria) small value. An initial guess can be provided or simply set to zero (solving the uncoupled problem), and each new set of {Y} values can then be used to modify the nonlinear [A] matrix (or the {B} vector). This method has been used to solve several nonlinear differential equations with a great deal of success, and achieving convergence in usually five or six iterations.

4.2 Fourth-order Transfer-matrix Error Estimate

Since the above solution method involves a fourth-order Runge-Kutta integration which is an application of a fourth-order Taylor series, the error induced in using the approximation can be estimated by evaluating the Taylor series remainder term [10]

$$e = \frac{h_i^4}{4!} \frac{d^4\{Y_i\}}{dx^4} \tag{4.14}$$

The fourth derivative of {Y} with respect to x can be evaluated by using the chain rule of calculus on equation (4.1).

CHAPTER 5

COMPUTER PROGRAMS

Two computer programs, written in the FORTRAN programing code on a personal computer, were developed to solve the equations developed in chapters 2 and 4. The first program, PROP, computes the cross-sectional properties for a thin open cross section; and the second program, SOLVE, solves the governing equations that are summarized in figure 3.1. Both of the programs were developed for the desk-top personal computer and were designed to run independent of each other; however, they are easily coupled through a data-base or spread-sheet program such as LOTUS-1-2-3.

5.1 Program PROP

Program PROP computes all of the required cross-sectional area properties that are described in chapter 2.4.2 by using the equations developed in appendix B. This program is written in FORTRAN-77 for the personal computer and can easily be up-loaded to a mainframe computer that uses a similar version of FORTRAN. The program only requires ordered pairs of coordinates that adequately define the upper and lower surfaces. These points need not be evenly spaced or have coincidence abscissa coordinates.

Figure 5.1 is a flowchart of the program PROP. The program, upon being started, reads from a user-defined file the upper and lower surface definitions. Next, the user is prompted to input the number of equally spaced integration points. This option is provided so that the user can determine if the numerical integration of the equations in appendix B have converged. The equal spacing of the integration points are determined by linearly interpolating between the input surface definitions. Thus, a reasonable description of the surfaces needs to be input. For the geometries considered in this analysis, the cross-sectional properties indicated convergences with 150 to 200 integration points. After the number of integration points has been determined, the program then computes the chord length and the n equally spaced stations. From this data, the area and shear center are computed, then the cross-section properties are computed about the shear center. The user is then prompted to input an angle about which the properties are to be transformed. The transformed properties are computed and printed, and the user is prompted to input more data. If more data are to be analyzed, the program is reinitialized and restarted.

5.2 Program Solve

The Hunter transfer-matrix method described in appendix A and the fourth-order matrices developed in chapter 4 have also been programed in FORTRAN-77 for the personal computer. This program yields a solution to the equation summarized in figure 3.1 using the boundary conditions in equations (3.17) and (3.18).

Figure 5.2 is a flowchart of the program SOLVE. This program requires as input the number of station and the properties shown in the matrices in figure 3.1 for each station that is defined. Upon starting the program, all inputs are read in a table format, and all undefined variables are set to zero. The program is initialized by setting the iteration counter to one and assuming all nonlinear variables are zero. This usually solves the linear uncoupled problem and is a reasonable estimate for the second iteration. The station matrices, [A] and {B}, are assembled in a user written subroutine that has been precompiled with the main program. Upon assembling the [A] and {B} matrices, the other system matrices are assembled. Then using the boundary condition, the first station is related to the last, resulting in a single linear matrix equation that requires solving. Once the complete solution at station one is known, then equation (A.11) is repeatedly applied until all of the $\{Y_j\}$'s have been found. Since the check values of the solution variables are preset to zero, the first convergence check always fails and the second iteration is automatically started. After the second iteration, subsequent iterations produce smaller and smaller errors until the convergence checks are satisfied. When convergence is achieved the solution is printed and the program terminated.

CHAPTER 6

RESULTS OF APPLICATION

To determine the effect of the centrifugal force stiffening on a rotating beam, two example cases are evaluated, each for a blade rotating at a constant angular speed of 475 revolutions per minute (RPM). The first case compares the transfer-matrix solution of the governing equations to a nonlinear finite-element analysis of a rotating 7- by 10-Foot Wind Tunnel fan blade that neglects the effects of the mass axis and elastic axis being eccentric. The second case includes the effect of the mass axis being eccentric from the elastic axis for the transfer-matrix solution and evaluates the influence of the nonlinear terms on the response.

6.1 Nonuniform, Noneccentric, Twisted Fan Blade

A special case of the fan blade geometry presented in appendix B where the mass axis eccentricity is neglected is analyzed using both finite elements and the transfer-matrix solution. Both models were analyzed using a set of steady aerodynamic design load that were developed by the Ames Research Center specifically for the 7- by 10-Foot Wind Tunnel fan blades.

6.1.1 Transfer-Matrix Solution

The equations that are summarized in figure 3.1 were solved using the program that is discussed in section 5.2 and the cross-sectional

properties summarized in appendix B. The steady aerodynamic loads shown in table 6.1 were assumed to act the quarter-chord point; and, therefore, had to be transferred to the elastic axis which resulted in a distributed torque along the blade in addition to the transverse loadings. A converged solution, following the flow-chart shown on figure 5.2, was achieved in seven iterations. Since the steady aerodynamic loadings were discontinuous at station 96, a double station was used at this station. This was accomplished easily by utilizing the feature of reducing the transfer matrix to an identity matrix when $h_i = 0$ (or a double station). Taking advantage of this precludes the solution algorithm from tapering the applied loading to zero from station-to station.

TABLE 6.1 - AERODYNAMIC DESIGN LOAD INTENSITIES

STATION (in)	AXIAL (lbs/in)	TANGENTIAL (lbs/in)
96	34.55	14.33
106	45.23	15.94
116	55.08	16.54
126	65.37	17.09
136	74.78	17.24
146	83.10	16.93
156	88.97	16.04
166	90.48	14.44
173	89.91	13.07

6.1.2 Nonlinear Finite-Element Solution

As a means of performing an accuracy check on the transfer-matrix solution, a finite-element model of the fan blade using two-noded beam elements and the EAL [12] finite-element computer code was analyzed on the CYBER CY17-855 mainframe computer. The finite-element analysis assumes the reference axis of the beam is the centroid axis while the transfer-matrix solution uses the elastic axis as the reference axis. To avoid over complication for a test case, the mass axis off-sets were neglected. This allowed the same loads to be input for both analysis without additional transformations, with the exception of the torque. The transverse loadings were input to the finite-element code as distributed load; however, no such feature exists for moments. This difficulty was overcome at the expense of inducing a small error by inputing the distributed torque as a discrete torque at each grid point. A similar approximation was induced by discretizing the geometry into elements with constant properties (the transfer-matrix solution assumes variable properties between stations). After defining the model and loads, the geometric nonlinear analysis (GNA) runstream element of EAL was modified to allow for the previous iteration's displacements to be used in computing the centrifugal forces due to the fan blade rotating at 475 rpm (49.742 rad/sec). Introducing this additional nonlinearity, resulted in the EAL code requiring 31 iterations before convergence was achieved.

6.1.3 Transfer-Matrix and Finite-Element Solution Comparison

The solution results for the finite-element and transfer-matrix methods are compared. This method of validating the transfer-matrix

method for the rotating beam problem was selected due to the absence of any experimental or analytical data in the literature. All of the studies that were surveyed were centered around predicting and correlating the natural frequency response (frequency and mode shapes) of a rotating beam. If any displacements and loads were computed, they were for a nonrotating propeller or fan blade under static loads.

The two solution methods could not be compared directly on all responses due to the basic formulation differences. Comparisons are made on the displacements, rotations, twist, and support reactions. Internal loads could not be compared due to the finite-element approach of discretizing variable properties. However, all of the other quantities were compared. Support reactions for both solution methods are shown in table 6.2; these results indicate that there is a excellent agreement between the two methods. The largest percentage difference was in the twisting moment (only 2.1 percent). This is expected since the pretwist of the blade is explicitly accounted for in the transfer-matrix method, and is only approximately accounted for in the finite-element solution by transforming the principal axes of the cross section for an element. The displacement results (figures 6.1 through 6.6) with the exception of the axial displacement, figure 6.1, of the blade, agree extremely well. What is seen here is the primary difficulty of using finite-elements to solve this type of problem. The application of the centrifugal force, using finite elements, results in the inertial force (a function of mass, location, and deformations) becoming a lumped nodal quantity which at the stress-free end of the blade (tip) is not stress free. Because of

this condition, the displacement quantities at the end of the blade using finite elements may be in error.

TABLE 6.2 - SUPPORT REACTION COMPARISON

REACTION TYPE	FINITE ELEMENT RESULTS	TRANSFER MATRIX RESULTS	PERCENT DIFFERENCE
T (lbs)	173,205	173,835	- 0.4
V_y (lbs)	- 1,455	- 1,447	0.5
V_z (lbs)	5,382	5,382	- 0.0
M_x (in-lbs)	33,911	34,632	- 2.1
M_y (in-lbs)	-367,055	-372,021	- 1.3
M_z (in-lbs)	- 82,547	- 82,980	- 0.5

With the noted exceptions, the finite-element and transfer-matrix solution method agreement is good; thus, this comparison is considered to verify the transfer-matrix solution of the governing differential equations for a rotating beam.

6.2 Nonuniform, Eccentric, Twisted Fan Blade

After verifying the solution method, the fan blade model that was used in section 6.1 was modified to include the offset of the mass axis from the elastic axis. The solutions for the fully coupled case (the case where the full set of equations as indicated in figure 3.1 are utilized) and the partially coupled case (the case where all displacement nonlinearities are neglected) are compared. This comparison

illustrates the influence of the displacement nonlinearities that are indicated in figure 3.1.

6.2.1 Fully Coupled Transfer-Matrix Solution

The next solution that is performed is for the fully coupled, nonlinear, nonhomogeneous differential equations. This represents the design operating condition for the 7- by 10-Foot Wind Tunnel fan blades. The steady-state aerodynamic loads at the quarter-chord point are shown in table 6.1; these loads as indicated in section 6.1.1 are transformed to the elastic axis. By including all of the displacement nonlinearities and the mass axis eccentricity, the solution converged in 12 iterations.

6.2.2 Partially Coupled Transfer-Matrix Solution

To determine the influence of the nonlinear terms shown in figure 3.1, all of the nonlinear terms that involve displacement and rotation terms are neglected; this leaves only the centrifugal axial force, T, coupling term in the bending moment equations. Neglecting the nonlinear displacement terms, the solution converged in three iterations. This is easy to see by noting that the axial force, T, equation is weakly coupled to the other equation through the axial displacement. The axial displacement term is usually neglected [2], and, therefore should have little influence on the net axial force solution. Thus, the axial force solution is nearly exact as a result of the first iteration; and upon using the first iteration's results in the second (neglecting the nonlinear displacement terms) the second iteration should result in a reasonable accurate solution. The third

iteration is used to insure that the absolute value of the difference between successive iterations is less than the required criteria.

6.2.3 Fully Coupled and Partially Coupled Transfer-Matrix Solution Comparisons

Since the number of interations that were required to achieve a converged solution were found to vary drastically when the displacement nonlinear-terms were considered, a comparison of the solutions is made. The more notable effects of these nonlinear terms were observed to influence the displacements and rotations, and had little or no effect on the forces and moments.

A comparison of the axial displacement is shown in figure 6.7. The inclusion of the nonlinear displacement terms has a stiffening effect that reduce the tip displacement by approximately 25 percent; this is due to the blade not untwisting as much when the nonlinear terms are included.

By considering the nonlinear displacement effects on the transverse deflections (figures 6.8 and 6.9), the deflections increased on the order of 3 percent. This indicated an insignificant softening of the fan blade.

The most significant effect on the response is noted when the cross-sectional twisting of the fan blade is evaluated. This effect is essentially an order of magnitude stiffer, see figure 6.10. It is probably for this reason alone that these terms are necessary to include in performing a loads analysis of a rotating fan blade. For this analysis, the aerodynamic loadings were considered to remain constant and independent of the deformed shape of the blade.

Normally, however, this is not the case, since the aerodynamic loadings are generally a function of the angle-of-attack of the blade (relative to the free-stream). The lift and drag loads are then displacement dependent. If the aerodynamic loads are a function of the blade's displacements, then this condition can be included by introducing an additional nonlinear term in the load vector which is iterated along with the other terms or by reformulating the problem as a beam on an elastic foundation and including the displacement dependent loads as linear terms in the A-matrix.

Like the transverse displacements, the bending rotations, by including the nonlinear terms, demonstrates a softer response, see figures 6.11 and 6.12 for this effect. These terms are strongly coupled in the moment equations to the mass axis eccentricities, and therefore would be expected to influence the solution.

Unlike the displacement results, the internal equilibrium loads are not strongly affected by the presence of the nonlinear displacement term. Figures 6.13 through 6.18 show little or no change in the load results. In fact with the exception of the transverse shear, V_y, and beam bending moment, M_z, (figures 6.14 and 6.18) plots of the two solutions completely overlay each other. These two loads are coupled and influenced by the y-inertial force component which, according to equation 2.43, is dependent upon the v transverse displacement and accounts for this small variation.

CHAPTER 7

CONCLUDING REMARKS

Nonlinear equations of motion for the coupled elastic bending and torsion of twisted nonuniform rotating beams are derived. In addition, a transfer-matrix solution method to solve these nonlinear equations is developed and presented. Two case were evaluated. The first case compares the transfer-matrix solution method to results obtained from a nonlinear finite-element code.

The nonlinear equations were developed by neglecting all but the first-order terms for the strain, and retaining all other nonlinear terms in the derivation. The resulting equations are for the coupled bending-torsion steady-state response of beams rotating at a constant angular velocity in a fixed plane.

The modified Hunter transfer-matrix method was verified by comparing results with solutions from a geometric nonlinear finite-element computer code. These results were shown to agree quite well, and that as is the case with any special purpose analysis when compared with a general purpose code, the transfer matrix yielded a more accurate representation and solution of the problem. An analysis of a proposed new fan blade design for the 7- by 10-Foot Wind Tunnel at the Langley Research Center was performed, and the effect of including nonlinear displacement terms on this solution addressed.

As a result of performing this analysis, two computer codes were developed for a desk top personal computer. The first program is a general purpose two-point boundary value problem solver that was used to solve the nonlinear, coupled governing differential equations of motion for a rotating beam. The second program performs a numerical integration for the cross-section properties for a thin open cross section that can be defined by an upper and lower surface.

This thesis develops the effective and efficient analysis techniques that consider the unique features common to rotating systems to determine the steady-state response of rotating blades.

REFERENCES

1. Houbolt, J. C.; and Brooks, W.: Differential Equations of Motion for Combined Flapwise Bending, Chordwise Bending, and Torsion of Twisted, Nonuniform Rotor Blades. NACA Report 1346, 1958.

2. Hunter, W. F.: Integrating Matrix Method for Determining the Natural Vibration Characteristics of Propeller Blades. NASA TN D-6064, 1970.

3. Stafford, R. O.; and Giurgiutiu, V.: Semi-Analytic Methods for Rotating Timoshenko Beams. Int. J. mech Sci. 17, 1975.

4. Oden, J. T.: Mechanics of Elastic Structures. McGraw-Hill, New York, 1967.

5. Myklestad, N. O.: A New Method of Calculating Natural Modes of Uncoupled Bending Vibration of Airplane Wings and Other Types of Beams. Jour. Aero Sci., April 1944.

6. Thomson, W. T.: Matrix Solution for the Vibration of Nonuniform Beams. J. Appl'd Mech., September 1950.

7. Pilkey, W. D.; and Chang, P. U.: Modern Formulas for Statics and Dynamics, McGraw Hill, New York, 1978.

8. Hildebrand, F. B.: Advanced Calculus for Application. Prentice Hall, Englewood Cliffs, New Jersey, 1962.

9. Thomson, W. T.: Vibration Theory and Application. Prentice Hall, Englewood Cliffs, New Jersey, 1965.

10. Baumeister, T.; Avallone, E. A.; and Baumeister, T., III: Marks' Standard Handbook for Mechanical Engineers. McGraw Hill, New York, 1978.

11. Roark, R. J.: Formulas for Stress and Strain. Fourth Edition, McGraw-Hill, New York, p. 197, 1978.

12. Wetstone, W. D.: EISI-EAL Engineering Analysis Language Reference Manual--EISI-EAL System Level 2091. Engineering Information Systems, Inc., July 1983. Statics and Dynamics, McGraw Hill, New York, 1978.

APPENDIX A

THEORETICAL DERIVATION OF THE HUNTER TRANSFER MATRIX METHOD

The method that is presented here is a solution procedure that was developed by Dr. William F. Hunter, and used by him for several years to solve various homogeneous and nonhomogeneous two-point boundary-value problems. Because to date the method has not been documented, it is developed in detail in this appendix and referred to as the Hunter method.

The development of the transfer matrix for the linear coupled matrix equation of the form

$$\frac{d\{Y\}}{dx} = [A]\ \{Y\} + \{B\} \qquad (A.1)$$

is described. By expressing the equations in matrix notation, utilizing the transfer matrix as an operator, and applying the boundary conditions, the coupled linear differential equations are solved completely in two passes over the solution domain. The first pass is to satisfy all of the boundary condition (natural and geometric) at the first station; and the second pass develops the solution at each station within the problem domain.

Consider a system of linear nonhomogeneous first-order differential equations that can be expressed in matrix notation as

$$\frac{d\{Y(x)\}}{dx} = [A(x)]\ \{Y(x)\} + \{B(x)\} \qquad (A.2)$$

defined on the closed interval $x_1<x<x_n$.

Using subscripts to denote stations and primes to denote differentiation with respect to x, equation (A.2) at station i ($x = x_i$) is written as

$$\{Y_i'\} = [A_i]\ \{Y_i\} + \{B_i\} \qquad (A.3)$$

The boundary conditions at the end-points ($x = x_1$ and $x = x_n$) are also expressed in matrix notation as

$$[C]\ \{Y_1\} = \{P\} \qquad (A.4)$$

$$[D]\ \{Y_n\} = \{Q\} \qquad (A.5)$$

Approximating the value of {Y} at the station (i+1) as follows

$$\{Y_{i+1}\} = \{Y_i\} + \frac{1}{2} h_i\ (\{Y_i'\} + \{Y_{i+1}'\}) \qquad (A.6)$$

where

$$h_i = x_{i+1} - x_i \qquad (A.7)$$

then equation (A.2) may be written at station (i+1) and substituted along with equation (A.3), into equation (A.6) to give

$$\{Y_{i+1}\} = \{Yi\} + \frac{h_i}{2} ([A_i]\ \{Y_i\} + \{B_i\} + [A_{i+1}]\ \{Y_{i+1}\} + \{B_{i+1}\}) \qquad (A.8)$$

Now, the Y_{i+1} term on the right-hand side of equation (A.8) may be approximated by using a Taylor series expansion about Y_i. Retaining only those terms up through the first derivative, Y_{i+1} becomes

$$\{Y_{i+1}\} = \{Y_i\} + \{Y_i'\}$$

or

$$\{Y_{i+1}\} = \{Y_i\} + ([A_i]\ \{Y_i\} + \{B_i\}) \tag{A.9}$$

Substituting equation (A.9) into equation (A.8) gives

$$\{Y_{i+1}\} = \left([I] + \frac{h_i}{2}([A_i] + [A_{i+1}]) + \frac{h_i^2}{2}[A_{i+1}]\ [A_i]\right)\{Y_i\}$$

$$+ \frac{h_i}{2}(\{B_i\} + \{B_{i+1}\}) + \frac{h_i^2}{2}\ [A_{i+1}]\ \{B_i\} \tag{A.10}$$

where [I] is the identity matrix. It can be shown that the above result is a second-order Runge-Kutta integration (see ref. 8) for a system of equations expressed in matrix form.

Equation (A.10) may be rewritten as

$$\{Y_{i+1}\} = [E_i]\ \{Y_i\} + \{F_i\} \tag{A.11}$$

where

$$[E_i] = [I] + \frac{h_i}{2}([A_i] + [A_{i+1}]) + \frac{h_i^2}{2}[A_{i+1}]\ [A_i] \tag{A.12}$$

$$\{F_i\} = \frac{h_i}{2}(\{B_i\} + \{B_{i+1}\}) + \frac{h_i^2}{2}[A_{i+1}]\ \{B_i\} \tag{A.13}$$

The matrix $[E_i]$ is known as a transfer matrix, since it relates the values of the state variables at station (i+1) to those at the station i The transfer-matrix approach is often used to determine the natural vibration characteristics of beams However, for a nonhomogeneous system of equations, the solution is complicated by the appearance of the matrix $\{F_i\}$ in equation (A 11) Because of $\{F_i\}$, an approach much different from that of the natural vibration (homogeneous) problem is needed to relate the conditions at one boundary to those at the other boundary It is at this point that the shooting methods will iterate the equations until conditions at both boundaries are satisfied The Hunter transfer-matrix approach as outlined here eliminates this difficulty by employing a systematic application of equation (A 11) from one boundary to the other; thus, the boundary conditions are satisfied directly The development is easily seen by using equation (A 11) and expanding it out for a few intermediate stations between boundaries For example,

$$\{Y_2\} = [E_1]\{Y_1\} + \{F_1\}$$

$$\{Y_3\} = [E_2]\{Y_2\} + \{F_2\} = [E_2]([E_1]\{Y_1\} + \{F_1\}) + \{F_2\}$$

$$\{Y_4\} = [E_3]\{Y_3\} + \{F_3\} = [E_3]([E_2]([E_1]\{Y_1\} + \{F_1\}) + \{F_2\}) + \{F_3\}$$

Now, the above can be refactored, and $\{Y_i\}$ can be expressed in general as a function of $\{Y_1\}$ For example, the expression for $\{Y_4\}$ above becomes

$$\{Y_4\} = [E_3][E_2][E_1]\{Y_1\} + [E_3]([E_2]\{F_1\} + \{F_2\}) + \{F_3\}$$

In general, the relationship can be expressed as

$$\{Y_i\} = [G_i]\ \{Y_1\} + \{H_i\} \qquad (i=1,2,\ldots,n) \tag{A.14}$$

where

$$[G_i] = [E_{i-1}]\ [G_{i-1}] \qquad (i=2,3,\ldots,n)$$

$$[G_1] = [I] \tag{A.15}$$

$$\{H_i\} = [E_{i-1}]\ \{H_{i-1}\} + \{F_{i-1}\} \qquad (i=2,3,\ldots,n)$$

$$\{H_1\} = 0 \tag{A.16}$$

With equation (A.14), the state vector at one boundary can be related to the vector at the other boundary. Thus, equation (A.15) for i=n becomes

$$\{Y_n\} = [G_n]\ \{Y_1\} + \{H_n\} \tag{A.17}$$

The boundary conditions must be applied in order to determine $\{Y_1\}$. Equation (A.17) may be substituted into equation (A.5), and the results combined with equation (A.4) to give

$$\begin{bmatrix} [C] \\ \hline [D]\ [G_n] \end{bmatrix} \{Y_1\} = \begin{bmatrix} \{P\} \\ \hline \{Q\} - [D]\ \{H_n\} \end{bmatrix} \tag{A.18}$$

Since the coefficient matrix is nonsingular, equation (A.18) can be solved for $\{Y_1\}$. The solution for $\{Y_i\}$ (i>1) is obtained simply by applying equation (A.11) repeatedly.

It is worth emphasizing that the Hunter method, given above, does not require any iteration, and obtains the solution in a direct manner. As with other transfer matrix methods, very little computer

storage is needed. The method requires stepping through the problem domain from one boundary to the other twice. The first step-through is made to obtain $\{Y_1\}$, and the second step-through yields the solution.

Another feature is that the integration process conveniently handles any discontinuities in the physical properties (such as beam mass or stiffness, for example) of the problem by allowing double stations at any x_j (note that the transfer matrix $[E_j]$ reduces to the identity matrix for $h_j = 0$, see equation (A.12).)

APPENDIX B

CALCULATION OF 7- BY 10-FOOT WIND TUNNEL FAN BLADE SECTION PROPERTIES

In order to perform the analysis of the 7- by 10-Foot Wind Tunnel fan blade new design, the cross-sectional properties as defined by equations (2.65-74) need to be calculated about the shear center of a cross section relative to the beam's y-z coordinate system. (See figure 2.1.) Since the definition of a fan blade is usually given by coordinates that define the upper and lower surfaces, equations (2.65-74) can be rewritten in a form that will allow for numerical integration of the equations. The purpose of this appendix is to present the modified and transformed cross-section integral equations as well as the numerical results when applied to a new 7- by 10-Foot Wind Tunnel fan blade design.

A typical cross section of an airfoil-shaped fan blade and associated coordinate systems are shown in figure B.1. The cross-sectional coordinates of the lower (λ_ℓ) and upper (λ_u) surfaces are given in the $\psi - \lambda$ system. When the shear center is located, the $y_1 - z_1$ system is used to compute the section properties parallel to the $\psi - \lambda$ system but about the shear center (ψ_s, λ_s). Since a typical cross section can be twisted about the shear center relative to

the y-z system, the cross-sectional properties need to be transformed. The section properties transformed to the y-z system (shown in figures 2.1 and B.1) are then calculated.

Blade description data is assumed to be defined in the ψ - λ system. The area and shear center location are computed in this system by the following equations.

$$A = \int_0^c (\lambda_u - \lambda_\ell)\, d\,\psi \tag{B.1}$$

$$\psi_s = \frac{\int_0^c \psi(\lambda_u - \lambda_\ell)^3\, d\,\psi}{\int_0^c (\lambda_u - \lambda_\ell)^3\, d\,\psi} \tag{B.2}$$

$$\lambda_s = \left.\frac{(\lambda_u - \lambda_\ell)}{2}\right]_{\psi = \psi_s} \tag{B.3}$$

where c is the chord length.

Equation (B.2) is developed by considering equilibrium of a differential element under bending and requiring that the sum of the internal moments about the point called the shear center to vanish. Equation B.3 is an approximation that is used in this analysis for a thin airfoil shape.

The other section integrals are

$$\bar{y}_1 = \frac{1}{A} \int_0^c (\psi - \psi_s)\ (\lambda_u - \lambda_\ell)\ d\ \psi \tag{B.4}$$

$$\bar{z}_1 = \frac{1}{2} \int_0^c \left(\frac{\lambda_u^2}{2} - \lambda_s\ \lambda_u - \frac{\lambda_\ell^2}{2} + \lambda_s\ \lambda_\ell\right) d\ \psi \tag{B.5}$$

$$I_{y_1\ y_1} = \frac{1}{3} \int_0^c [(\lambda_u - \lambda_s)^3 - (\lambda\ell - \lambda_s)^3]\ d\ \psi \tag{B.6}$$

$$I_{z_1\ z_1} = \int_0^c (\psi - \psi_s)^2\ (\lambda_u - \lambda_\ell)\ d\ \psi \tag{B.7}$$

$$I_{y_1\ z_1} = \int_0^c (\psi - \psi_s)\ [(\lambda_u - \lambda_s)^2 - (\lambda_\ell - \lambda_s)^2]\ d\ \psi \tag{B.8}$$

$$\bar{P}_1 = \bar{y}_1\ A \tag{B.9}$$

$$\bar{P}_2 = \bar{z}_1\ A \tag{B.10}$$

$$\overline{P}_3 = \int_0^c \{[(\lambda_u - \lambda_s)^2 - (\lambda_\ell - \lambda_s)^2] \left(\frac{\psi - \psi_s}{2}\right)^2 + \frac{1}{4}[(\lambda_u - \lambda_s)^4 - (\lambda_\ell - \lambda_s)^4]\} \, d\psi \tag{B.11}$$

$$\overline{P}_4 = \int_0^c \{(\psi - \psi_s)^3 (\lambda_u - \lambda_\ell) + \left(\frac{\psi - \psi_s}{3}\right)[\lambda_u - \lambda_s)^3 - (\lambda_\ell - \lambda_s)^3]\} \, d\psi \tag{B.12}$$

$$\overline{P}_5 = \int_0^c \{(\psi - \psi_s)^4 (\lambda_u - \lambda_\ell) + \frac{1}{5}[(\lambda_u - \lambda_s)^5 - (\lambda_\ell - \lambda_s)^5] + \frac{2(\psi - \psi_s)}{3}[(\lambda_u - \lambda_s)^3 - (\lambda_\ell - \lambda_s)^3]\} \, d\psi \tag{B.13}$$

The torsional stiffness constant [11] can be calculated by

$$J = \frac{\frac{F}{3}}{1 + \frac{4F}{3Ac^2}} \qquad \text{where } F = \int_0^c (\lambda_u - \lambda_\ell)^3 \, dc \tag{B.14}$$

The following transformation rule relates the $y_1 - z_1$ system to the y-z system.

$$y = y_1 \cos(\beta_t) + z_1 \sin(\beta_t)$$
$$z = -y_1 \sin(\beta_t) + z_1 \cos(\beta_t) \qquad \text{(B.15)}$$

Using the transformation indicated in equation (B.15), the cross-section properties (equations (B.4-13)) in the y-z system become

$$y_m = \bar{y}_1 \cos(\beta_t) + \bar{z}_1 \cos(\beta_t) \qquad \text{(B.16)}$$

$$z_m = -\bar{y}_1 \sin(\beta_t) + \bar{z}_1 \cos(\beta_t) \qquad \text{(B.17)}$$

$$I_{yy} = I_{y_1 y_1} \cos^2(\beta_t) + I_{z_1 z_1} \sin^2(\beta_t) - 2 I_{y_1 z_1} \cos(\beta_t) \sin(\beta_t) \qquad \text{(B.18)}$$

$$I_{zz} = I_{y_1 y_1} \sin^2(\beta_t) + I_{z_1 z_1} \cos^2(\beta_t) + 2 I_{y_1 z_1} \cos(\beta_t) \sin(\beta_t) \qquad \text{(B.19)}$$

$$I_{yz} = I_{y_1 y_1} [\cos(\beta_t) \sin(\beta_t)] - I_{z_1 z_1} [\cos(\beta_t) \sin(\beta_t)] + I_{y_1 z_1} [\cos^2(\beta_t) - \sin^2(\beta_t)] \qquad \text{(B.20)}$$

$$P_1 = y_m A \qquad \text{(B.21)}$$

$$P_2 = z_m A \qquad \text{(B.22)}$$

$$P_3 = -\bar{P}_4 \sin(\beta_t) + \bar{P}_3 \cos(\beta_t) \qquad \text{(B.23)}$$

$$P_4 = \bar{P}_4 \cos(\beta_t) + \bar{P}_3 \sin(\beta_t) \qquad \text{(B.24)}$$

The properties, A, J, and P_5, are invarient, and, as such, they are not effected by coordinate transformations.

A sketch of a 7- by 10-Foot Wind Tunnel blade is shown in figure B.2. The stations indicated along the span of the blade are the points where the cross sections were cut and properties calculated. Figures B.3-18 show the cross section and indicates the cross-sectional properties in the y-z systems. For this analysis the fan blade from station 57.375 down toward the center of rotation was considered fixed due to the rigid attachment to two thick steel disks.

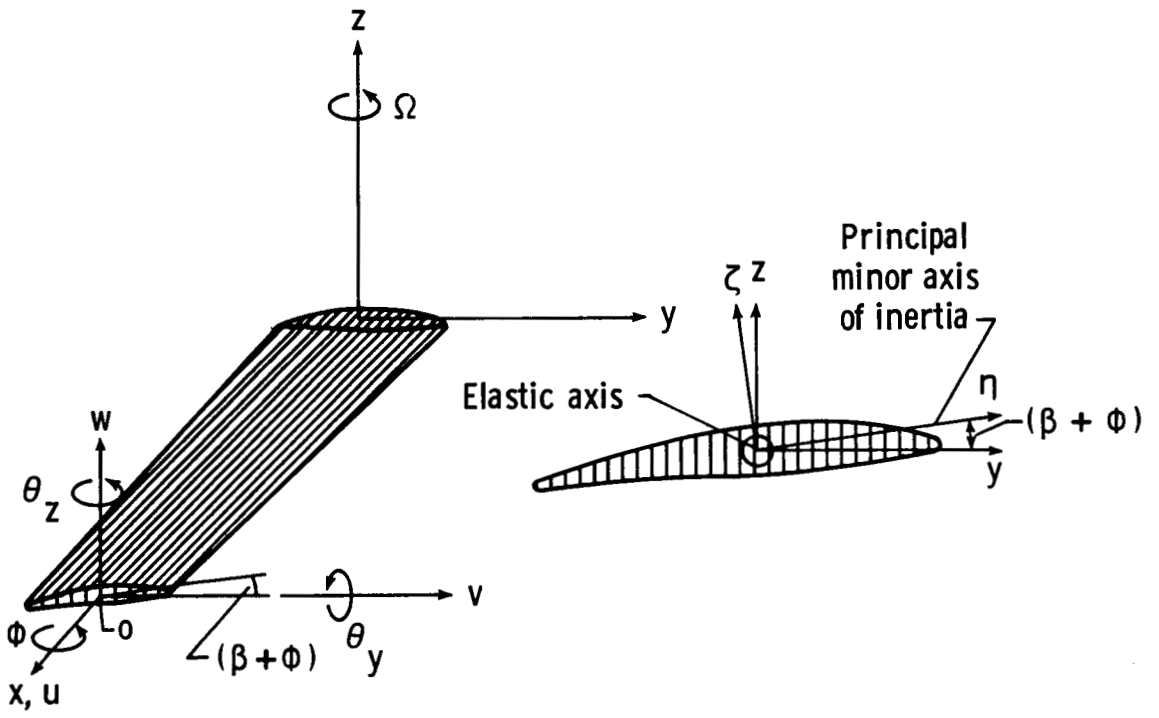

Fig 2.1 Geometry and sign convention of rotating beam

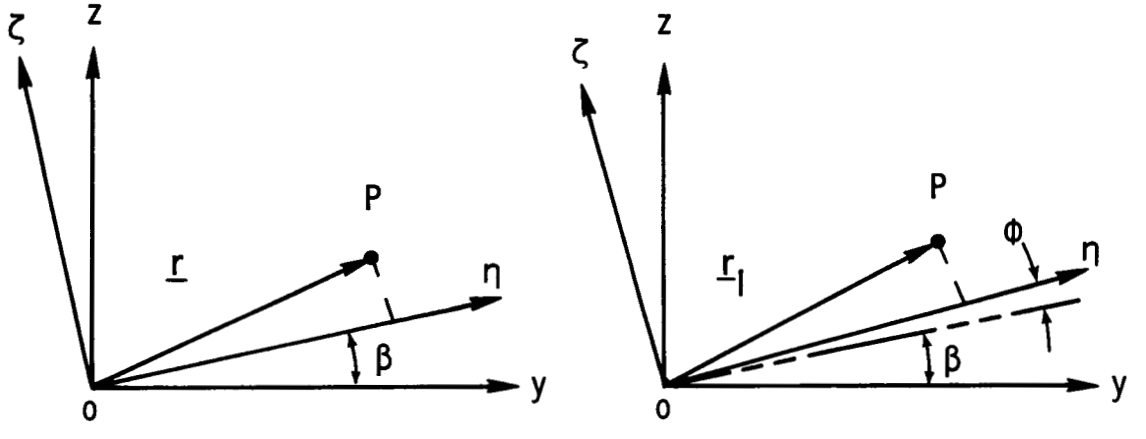

(a) Undeformed (b) Deformed

Fig 2.2 Cross-sectional geometry

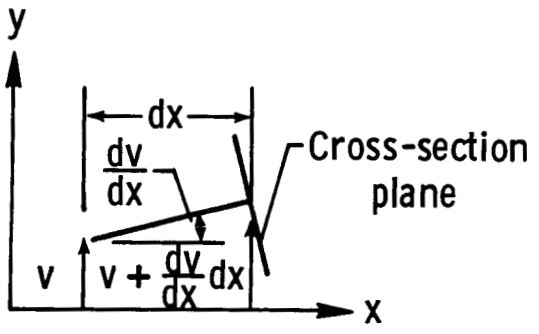

(a) Bending in the x-y plane

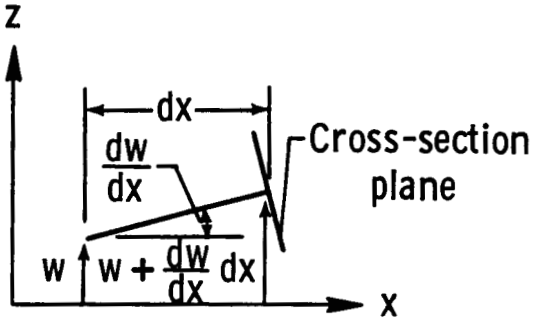

(b) Bending in the x-z plane

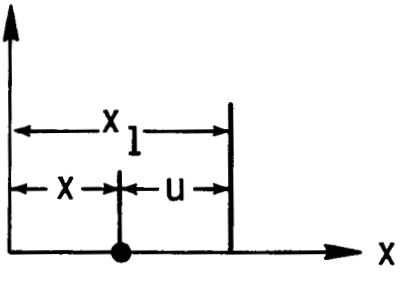

(c) Extension of elastic axis

Fig 2.3 Cross-sectional deformations

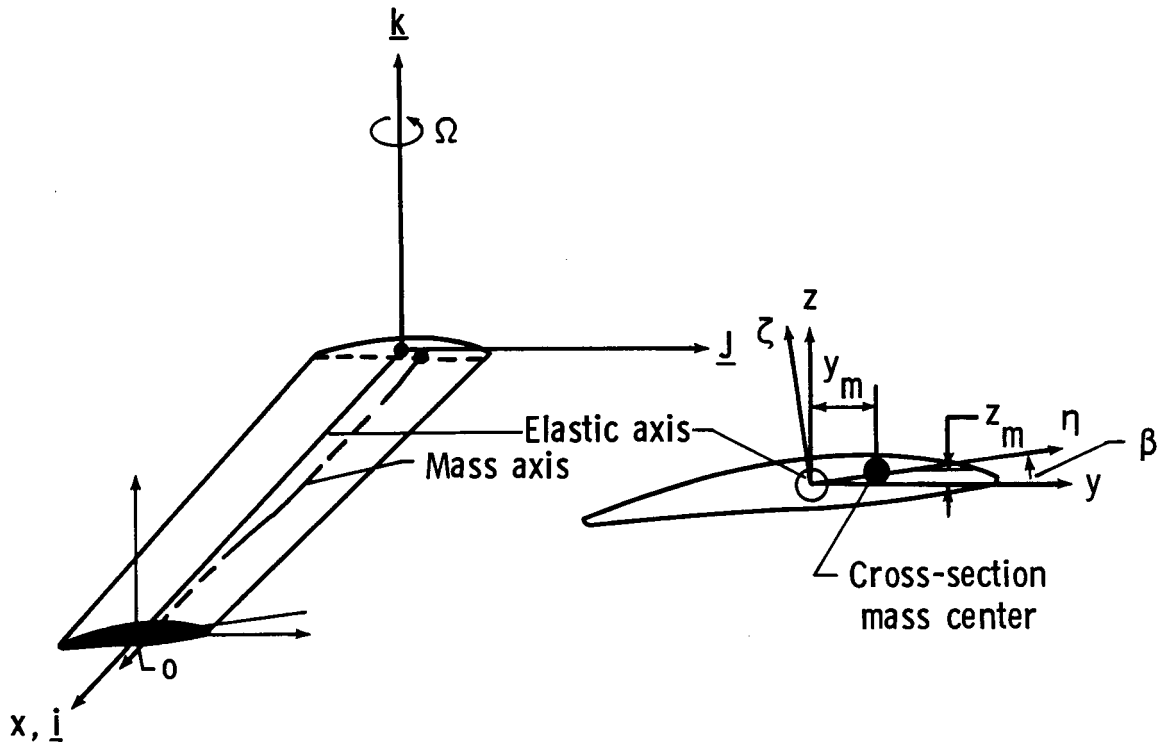

Fig 2.4 Orientation of rotating beam in undeformed configuration

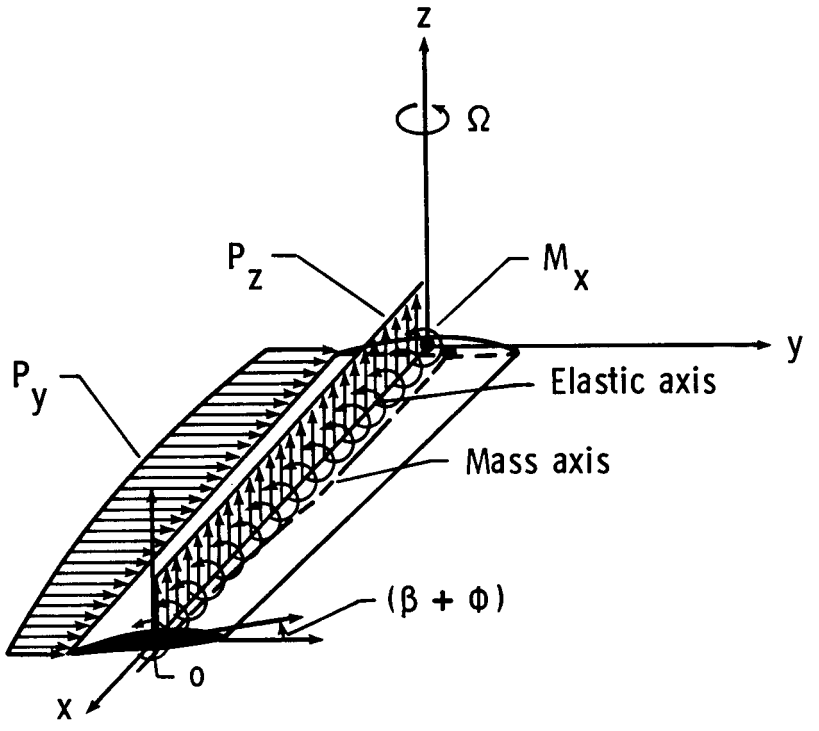

Fig 2.5 Rotating beam under steady-state aerodynamic loads

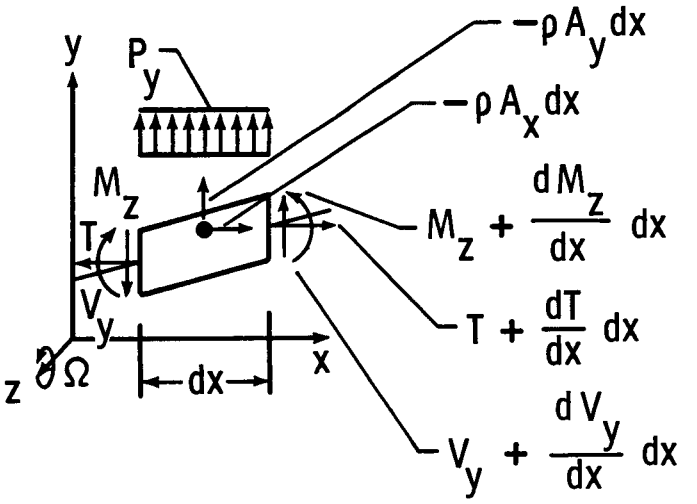

(a) x-y plane

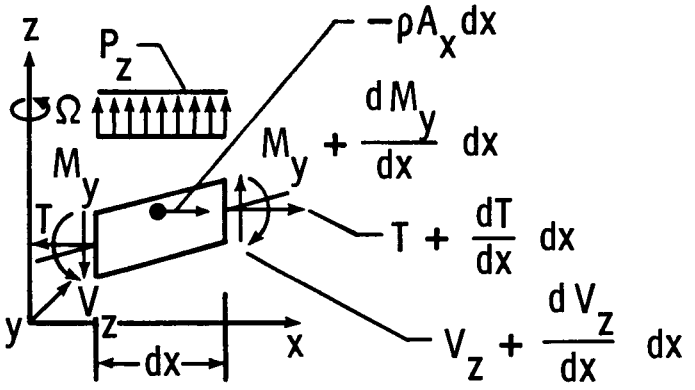

(b) x-z plane

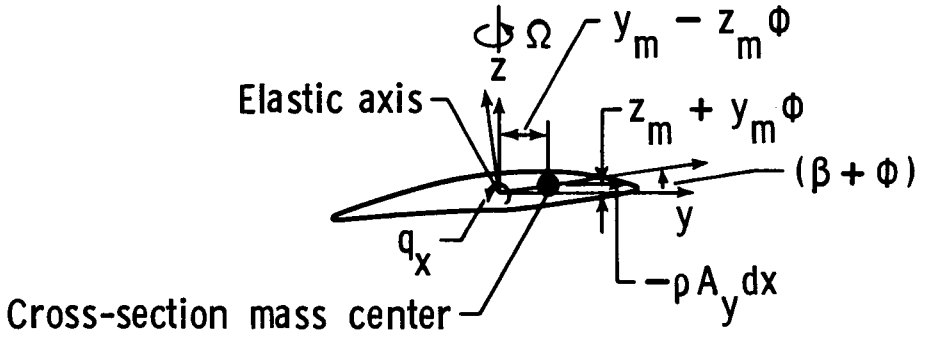

(c) y-z plane

Fig 2.6 Equilibrium of differential bending element

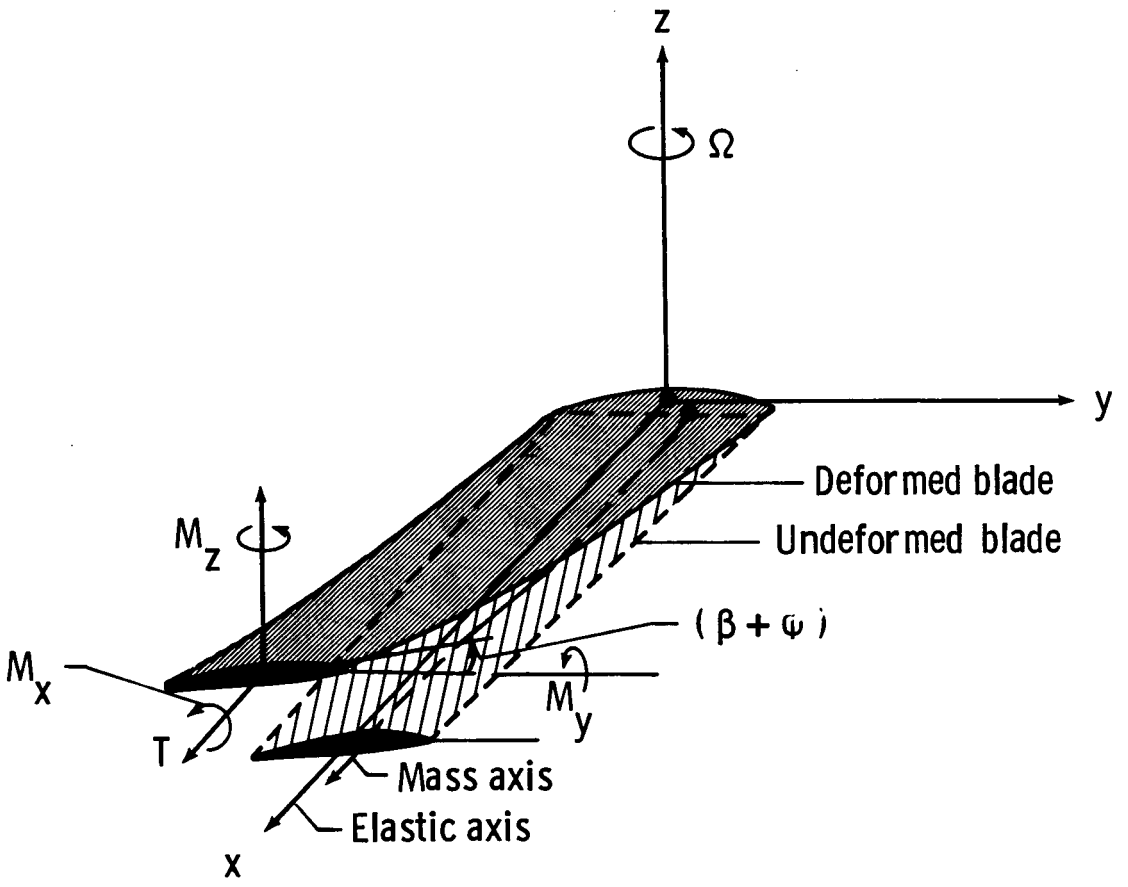

Fig 2.7 Internal elastic loads

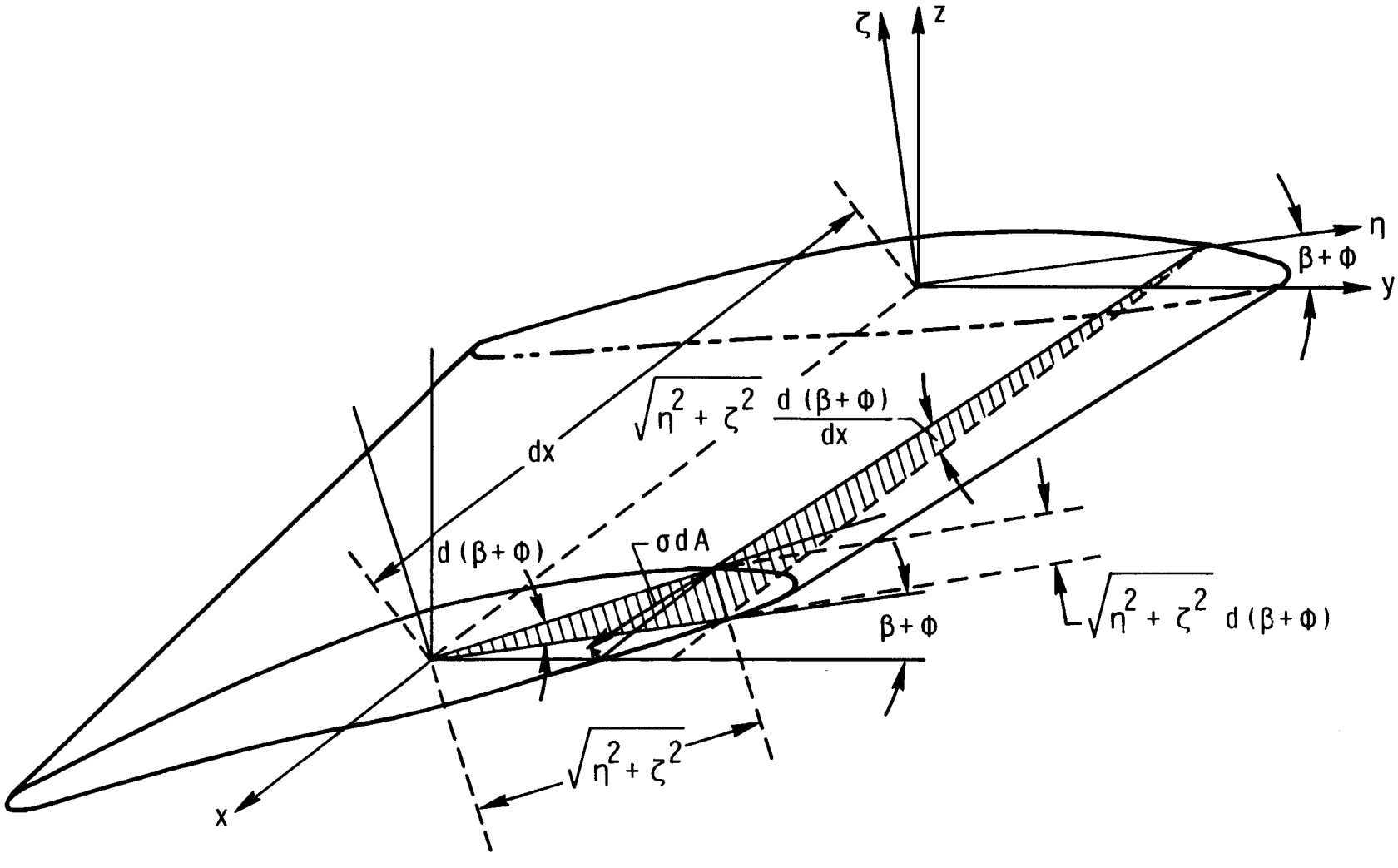

Fig 2.8 Contribution of longitudinal stress to the internal elastic torque

$$\frac{d\{Y\}}{dx} = [A]\{Y\} + \{B\}$$

$$\frac{d}{dx}\begin{Bmatrix} u \\ v \\ w \\ \Phi \\ \theta_y \\ \theta_z \\ T \\ V_y \\ V_z \\ M_x \\ M_y \\ M_z \end{Bmatrix} = \begin{bmatrix} 0 & 0 & 0 & 0 & 0 & 0 & ci_{11} & 0 & 0 & ci_{12} & ci_{13} & ci_{14} \\ 0 & 0 & 0 & 0 & 0 & 1.0 & 0 & 0 & 0 & 0 & 0 & 0 \\ 0 & 0 & 0 & 0 & -1.0 & 0 & 0 & 0 & 0 & 0 & 0 & 0 \\ 0 & 0 & 0 & 0 & 0 & 0 & ci_{21} & 0 & 0 & ci_{22} & ci_{23} & ci_{24} \\ 0 & 0 & 0 & 0 & 0 & 0 & ci_{31} & 0 & 0 & ci_{32} & ci_{33} & ci_{34} \\ 0 & 0 & 0 & 0 & 0 & 0 & ci_{41} & 0 & 0 & ci_{42} & ci_{43} & ci_{44} \\ -\rho\Omega^2 & 0 & 0 & 0 & -\rho\Omega^2 y_m & \rho\Omega^2 z_m & 0 & 0 & 0 & 0 & 0 & 0 \\ 0 & -\rho\Omega^2 & 0 & \rho\Omega^2 z_m & 0 & 0 & 0 & 0 & 0 & 0 & 0 & 0 \\ 0 & 0 & 0 & 0 & 0 & 0 & 0 & 0 & 0 & 0 & 0 & 0 \\ 0 & \rho\Omega^2 z_m & 0 & \rho\Omega^2\left(y_m^2 - z_m^2\right) & 0 & 0 & 0 & 0 & 0 & 0 & 0 & 0 \\ & & & + \rho\Omega^2 y_m v & & & & & & & & \\ & & & -\rho\Omega^2 y_m z_m \Phi & & & & & & & & \\ -\rho\Omega^2 z_m & 0 & 0 & -\rho\Omega^2 x_m y_m & T-\rho\Omega^2 z_m^2 & \rho\Omega^2 y_m z_m & 0 & 0 & 1.0 & 0 & 0 & 0 \\ & & & -\rho\Omega^2 y_m u & & & & & & & & \\ & & & + \rho\Omega^2 y_m^2 \theta_z & & & & & & & & \\ & & & + \rho\Omega^2 y_m z_m \theta_y & & & & & & & & \\ \rho\Omega^2 y_m & 0 & 0 & -\rho\Omega^2 x_m z_m & \rho\Omega^2 y_m z_m & T-\rho\Omega^2 y_m^2 & 0 & -1.0 & 0 & 0 & 0 & 0 \\ & & & -\rho\Omega^2 z_m u & & & & & & & & \\ & & & + \rho\Omega^2 y_m z_m \theta_z & & & & & & & & \\ & & & -\rho\Omega^2 z_m^2 \theta_y & & & & & & & & \end{bmatrix} \begin{Bmatrix} u \\ v \\ w \\ \Phi \\ \theta_y \\ \theta_z \\ T \\ V_y \\ V_z \\ M_x \\ M_y \\ M_z \end{Bmatrix} + \begin{Bmatrix} 0 \\ 0 \\ 0 \\ 0 \\ 0 \\ 0 \\ -\rho\Omega^2 x_m \\ -\rho\Omega^2 y_m - P_y \\ -P_z \\ \rho\Omega^2 z_m y_m - qx \\ -\rho\Omega^2 x_m z_m \\ \rho\Omega^2 x_m y_m \end{Bmatrix}$$

$$\begin{bmatrix} ci_{11} & ci_{12} & ci_{13} & ci_{14} \\ ci_{21} & ci_{22} & ci_{23} & ci_{24} \\ ci_{31} & ci_{32} & ci_{33} & ci_{34} \\ ci_{41} & ci_{42} & ci_{43} & ci_{44} \end{bmatrix} = \begin{bmatrix} EA & E\beta' I_p & EP_2 & -EP_1 \\ E\beta' I_p & \{GJ + C_\Phi\} & E\beta' P_3 & -E\beta' P_4 \\ EP_2 & E'\beta' P_3 & EI_{yy} & -EI_{yz} \\ -EP_1 & -E\beta' P_4 & -EI_{yz} & EI_{zz} \end{bmatrix}^{-1}$$

$$C_\Phi = E\left[I_p u' + P_3 \theta_y' - P_4 \theta_z' + P_5\left(\Phi' + |\beta'|^2\right)\right]$$

Fig 3.1 Governing differential equations in matrix format

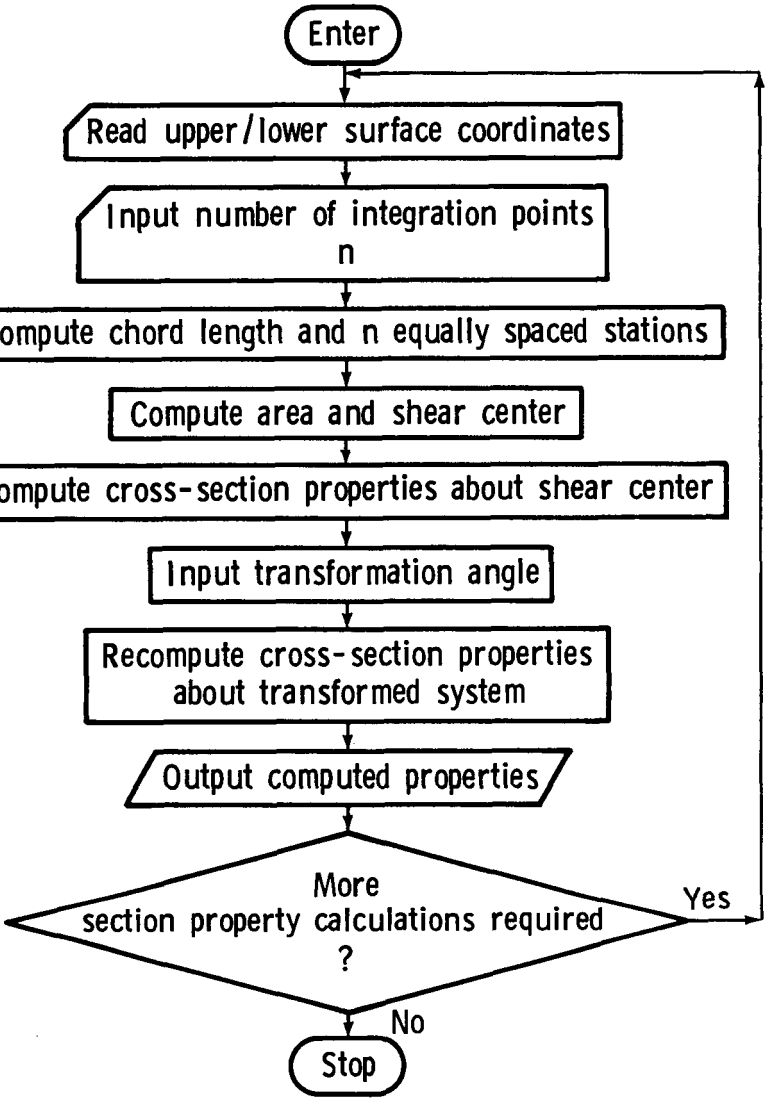

Fig 5.1 Flow chart of program PROP

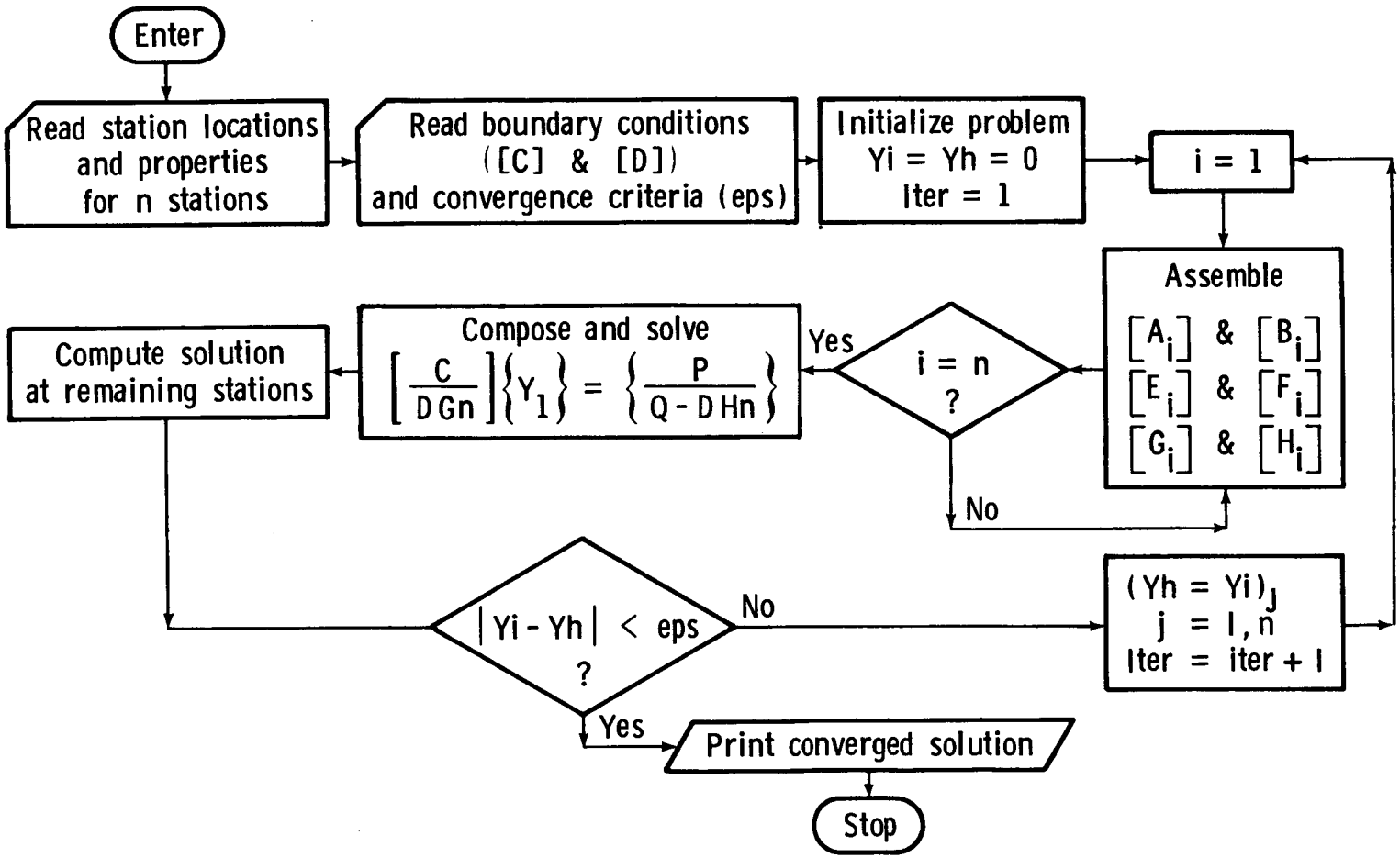

Fig 5.2 Flow chart of program SOLVE

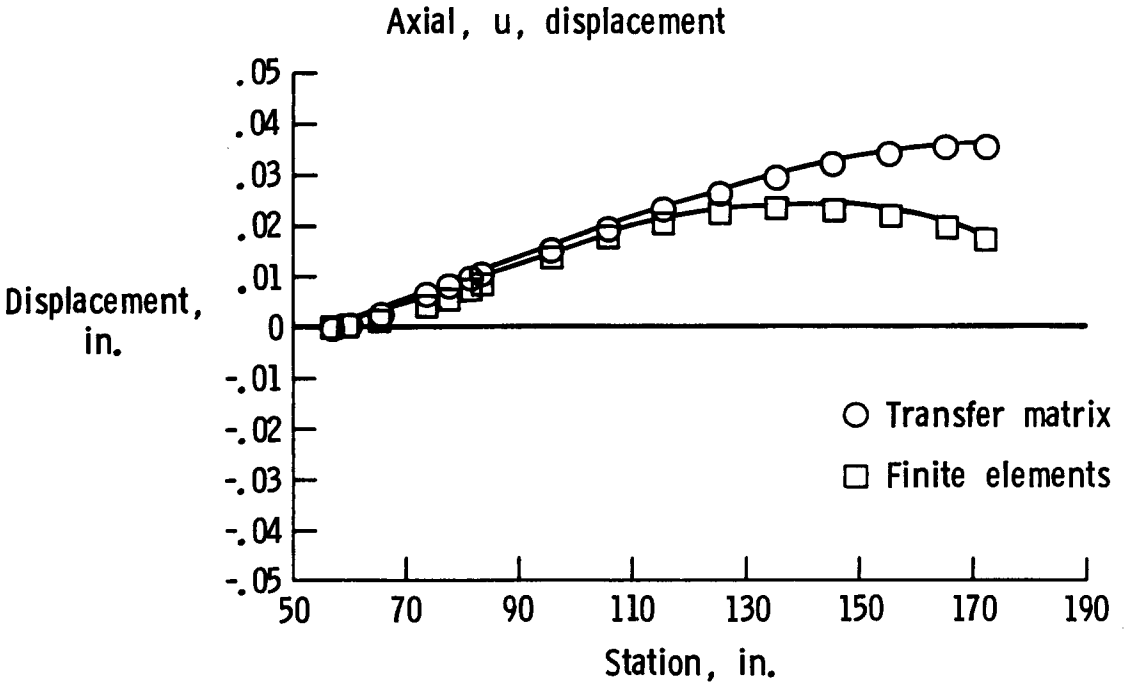

Fig 6.1 Comparison of axial displacements

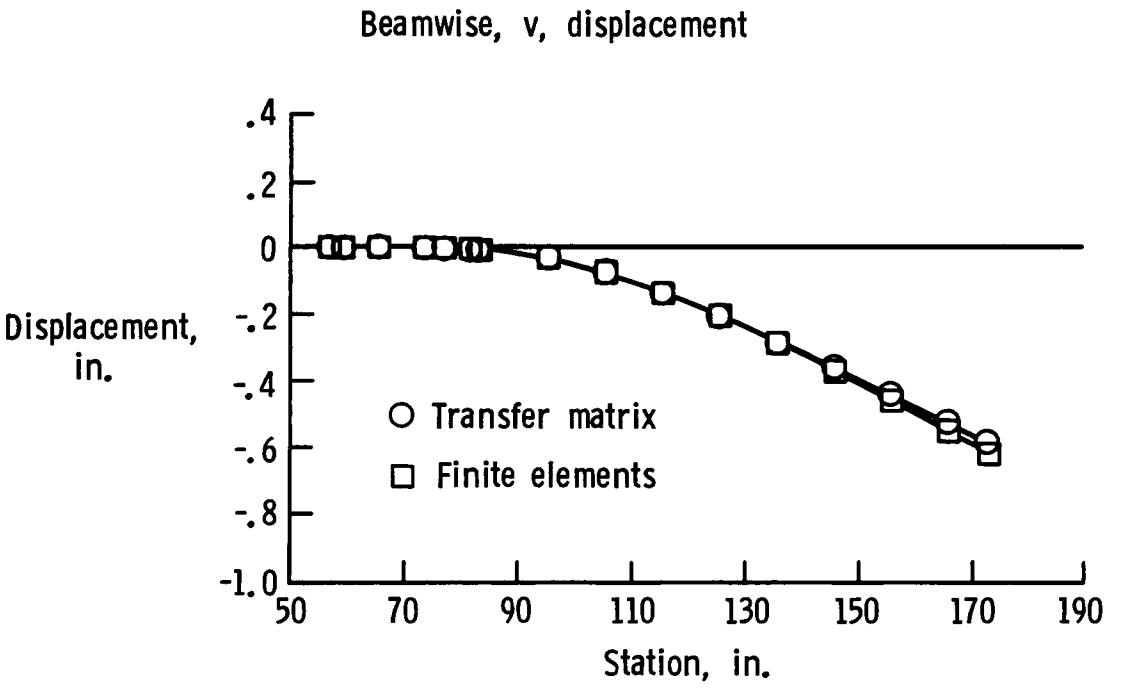

Fig 6.2 Comparison of beamwise displacement

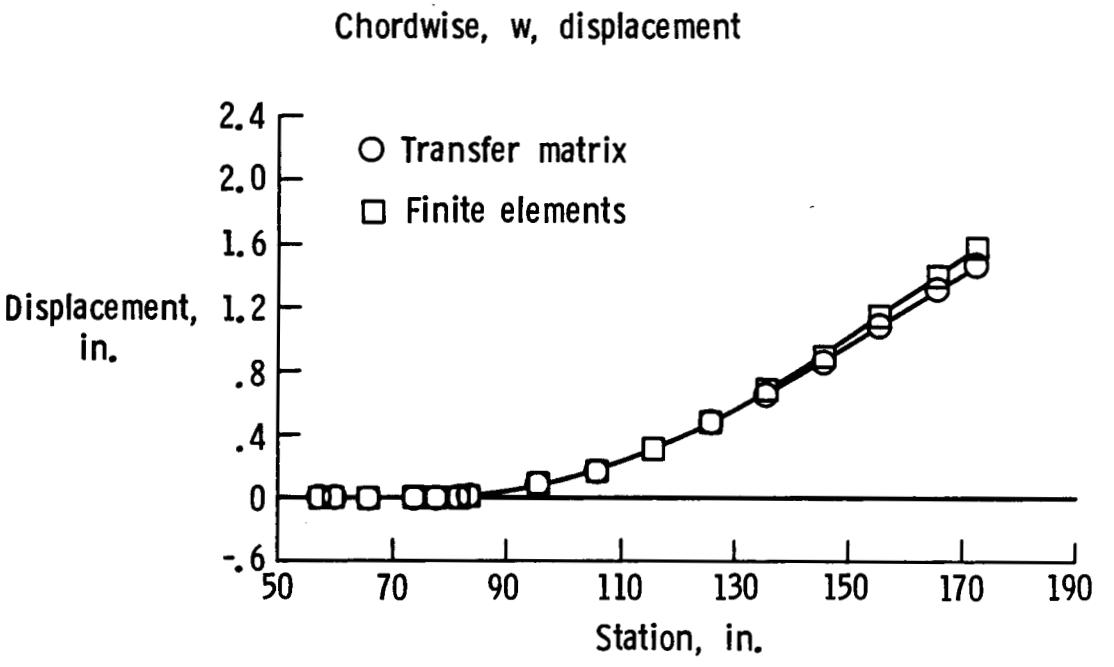

Fig 6.3 Comparison of chordwise displacements

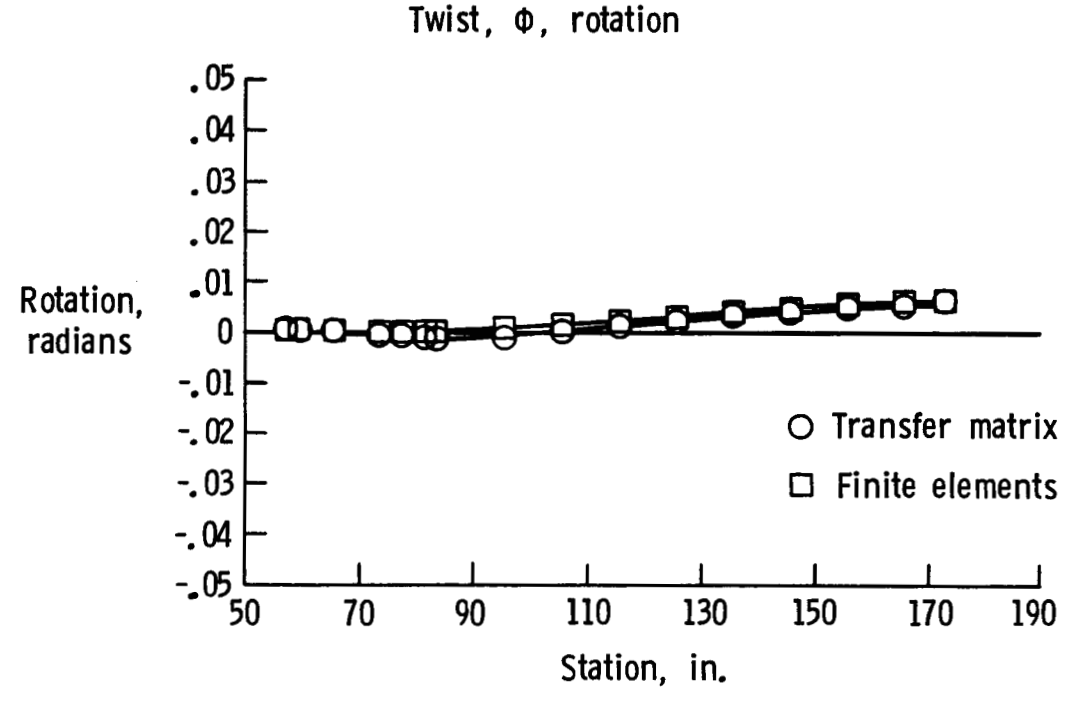

Fig 6.4 Comparison of cross-sectional twist

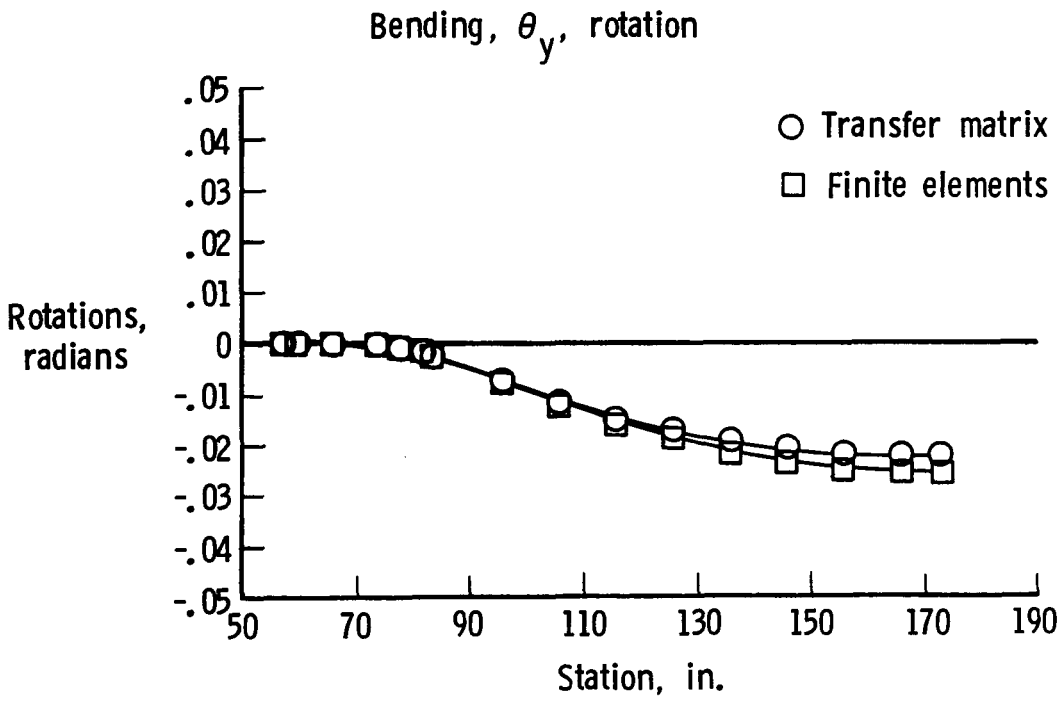

Fig 6.5 Comparison of θ_y rotations

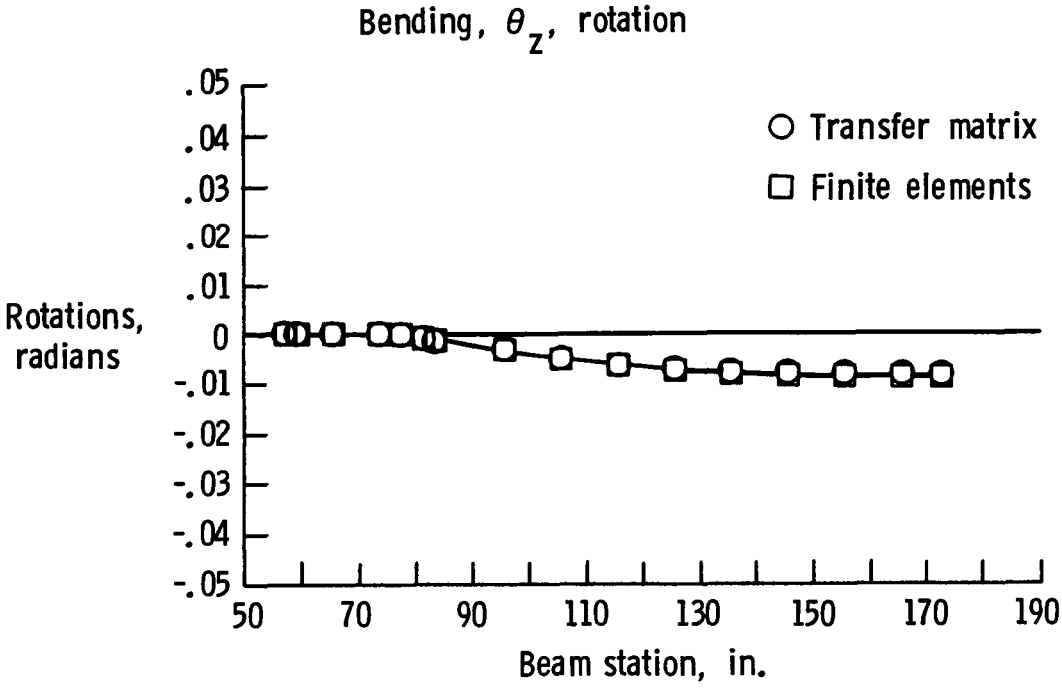

Fig 6.6 Comparison of θ_y rotations

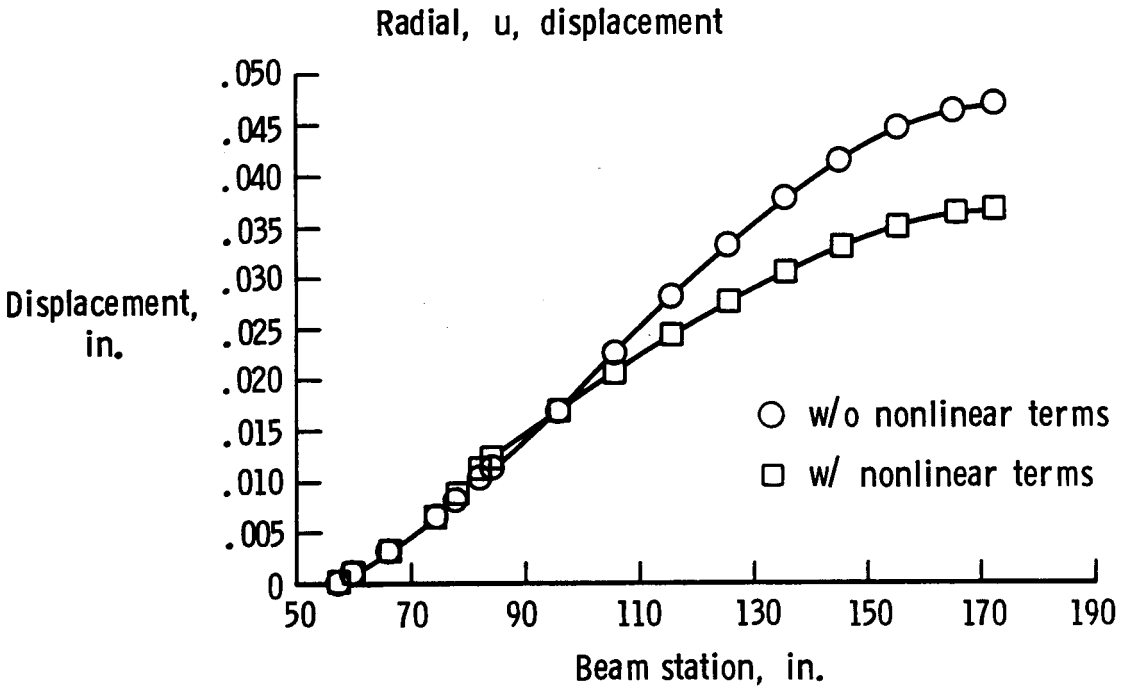

Fig 6.7 Axial displacement

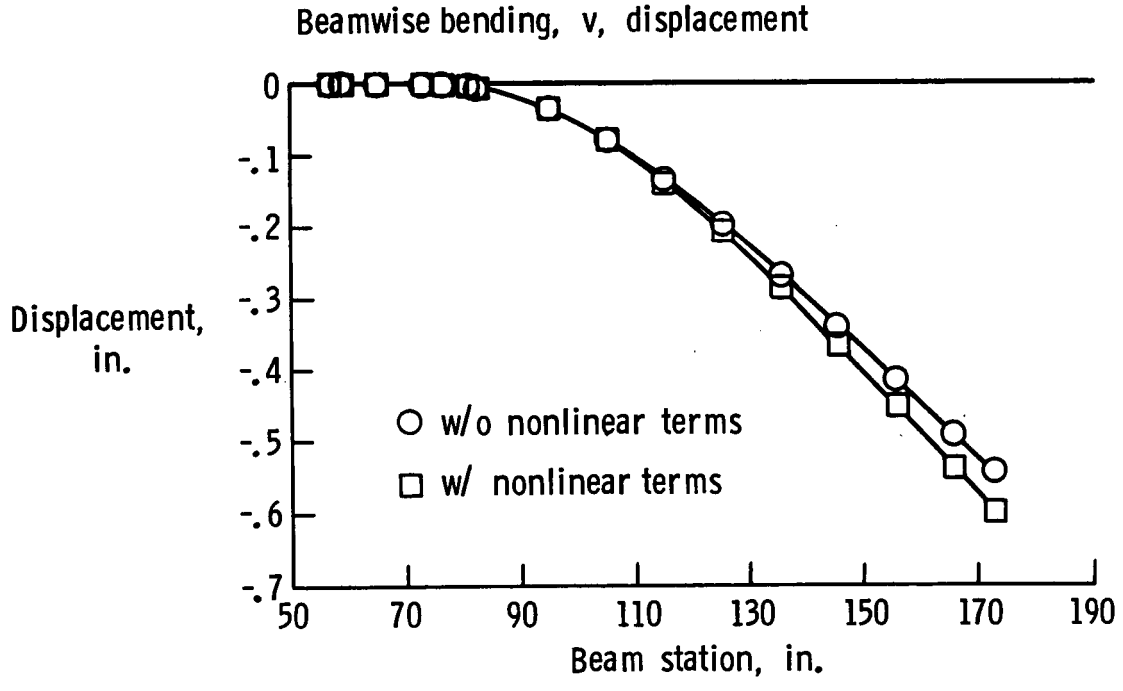

Fig 6.8 Beamwise transverse bending displacement

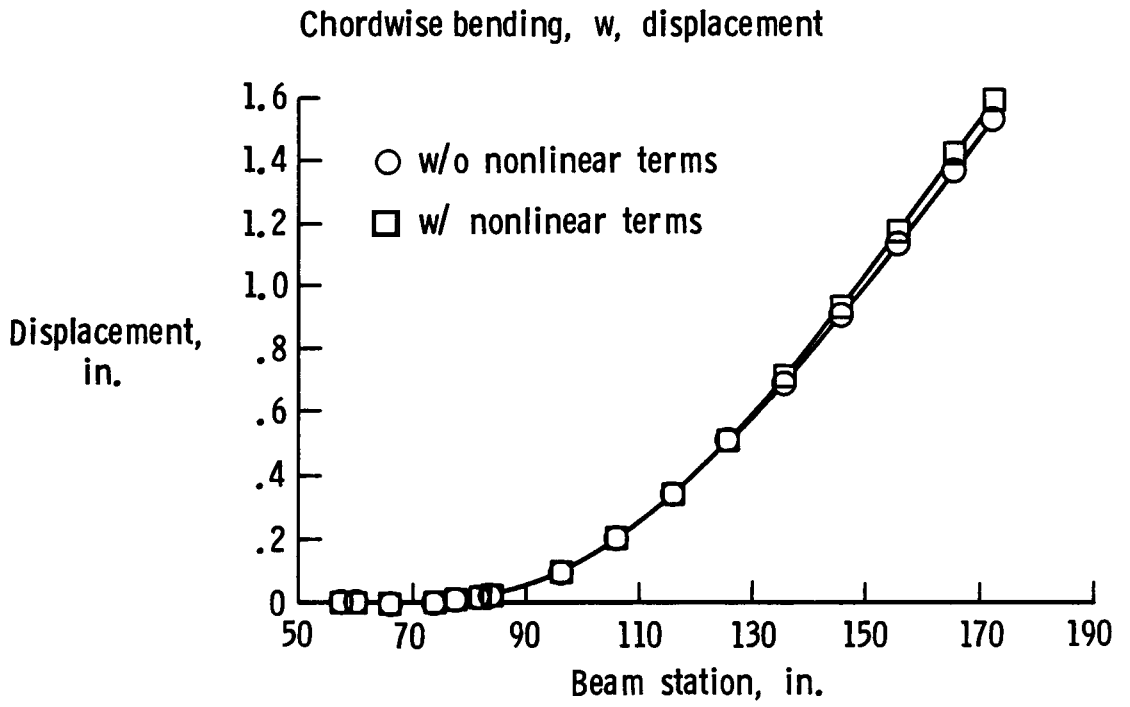

Fig 6.9 Chordwise transverse bending displacement

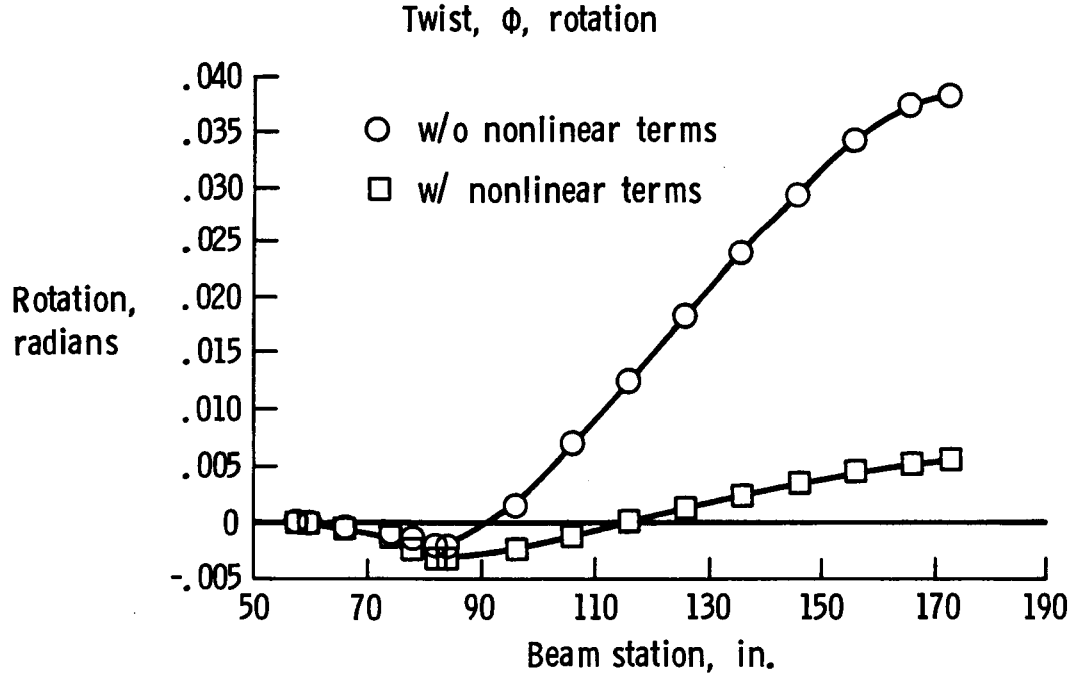

Fig 6.10 Beam twist, ϕ

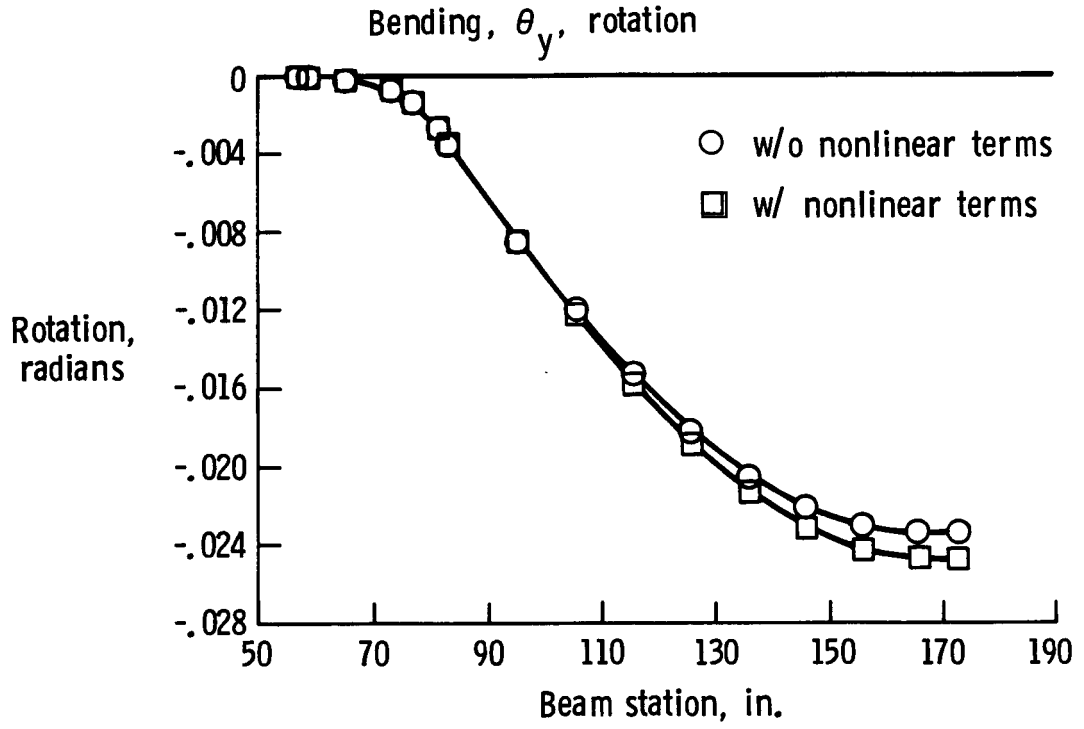

Fig 6.11 Bending rotation, θ_y

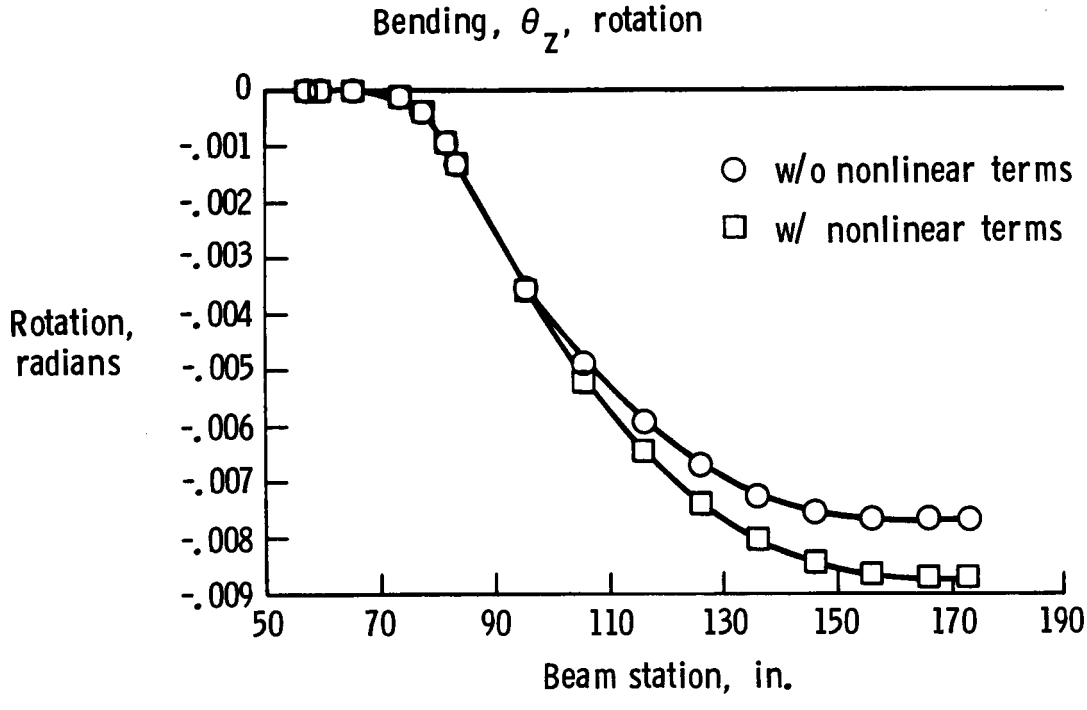

Fig 6.12 Bending rotation, θ_z

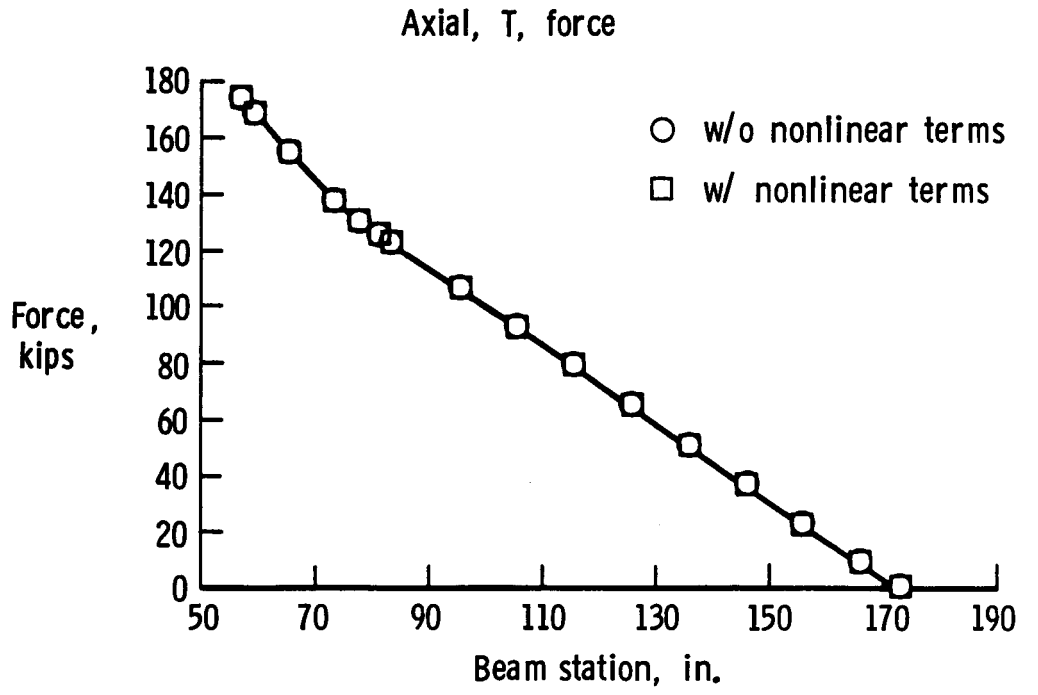

Fig 6.13 Axial force, T

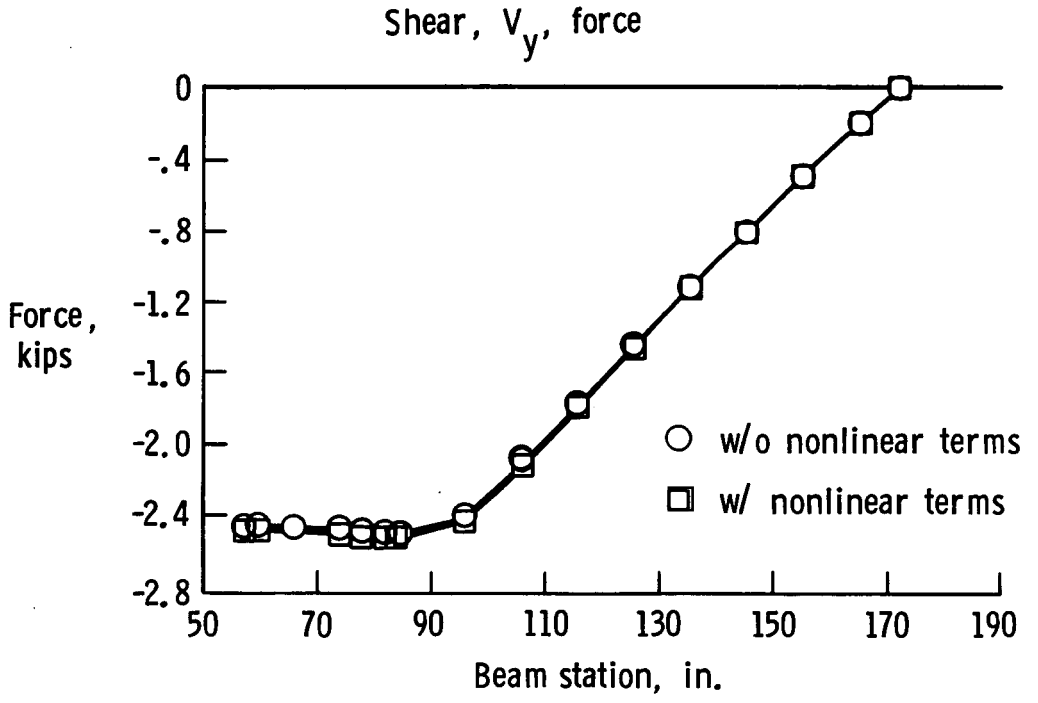

Fig 6.14 Beamwise shear force, V_y

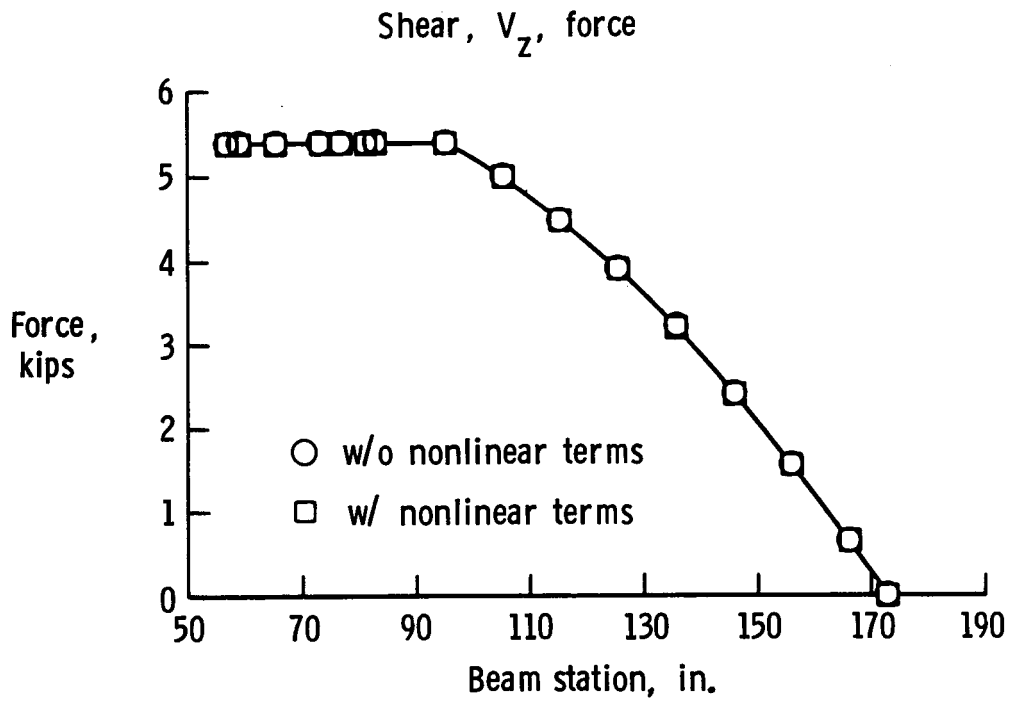

Fig 6.15 Chordwise shear force, V_z

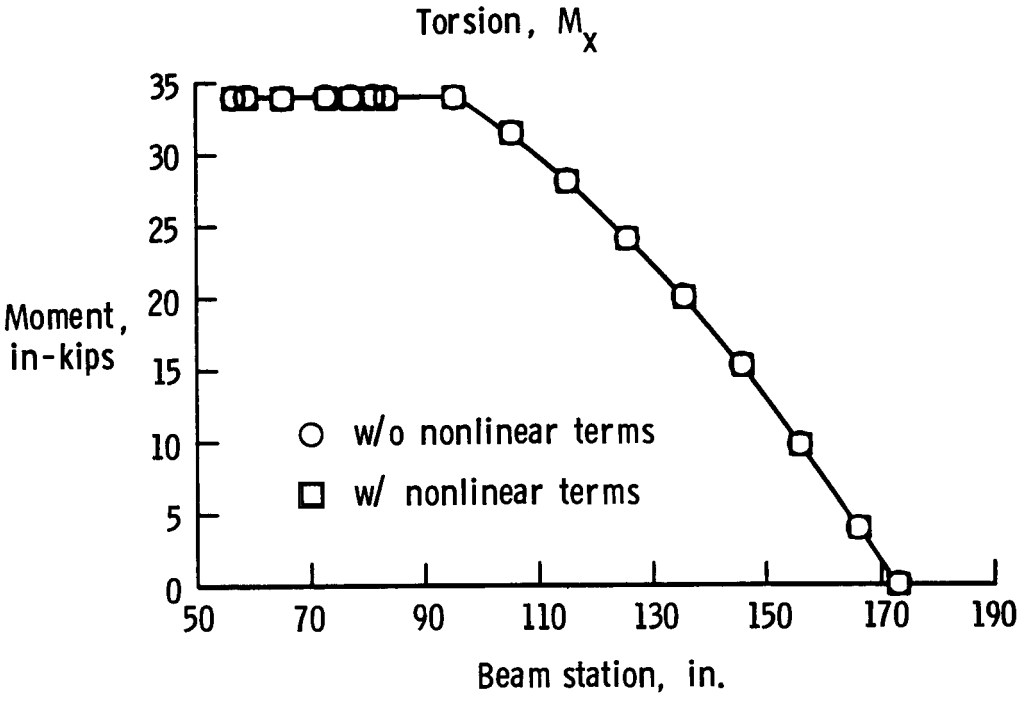

Fig 6.16 Twisting moment, M_x

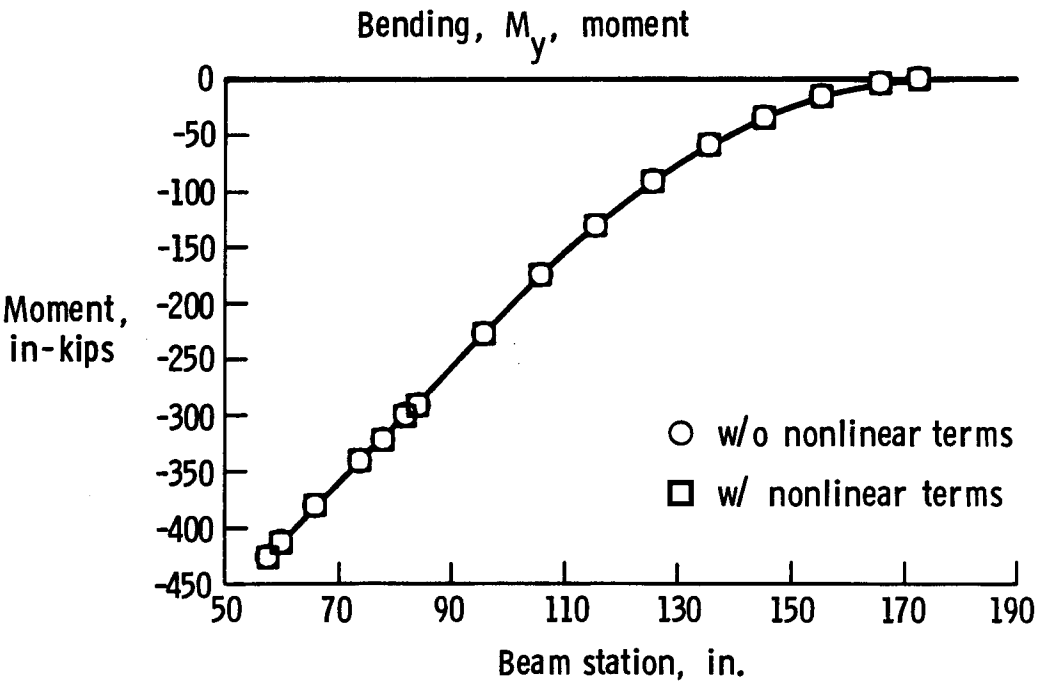

Fig 6.17 Beam bending moment, M_y

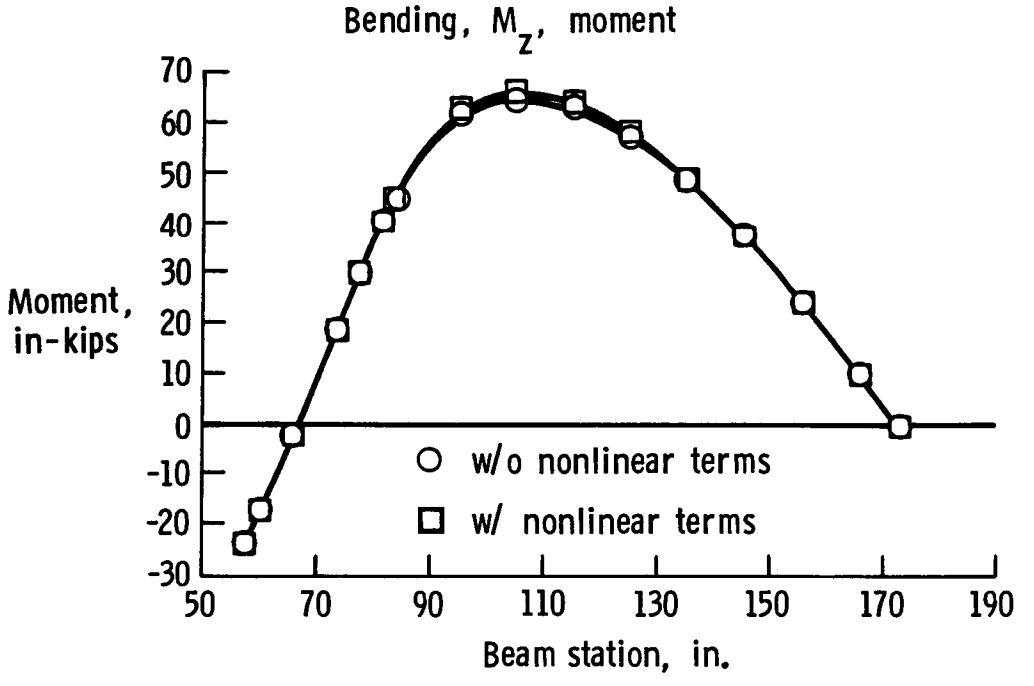

Fig 6.18 Beam bending moment, M_z

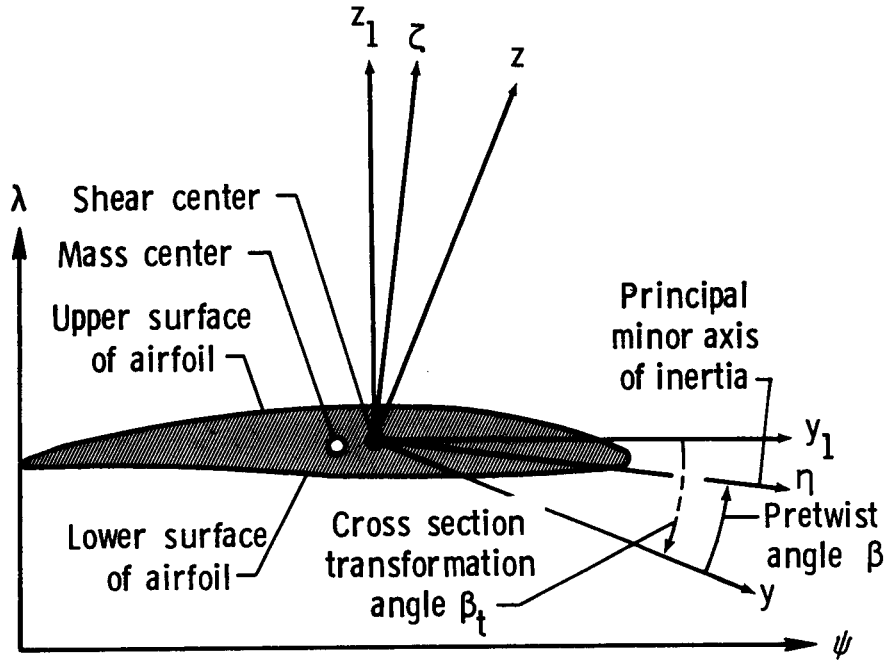

Fig B.1 Typical airfoil cross-sectional geometry

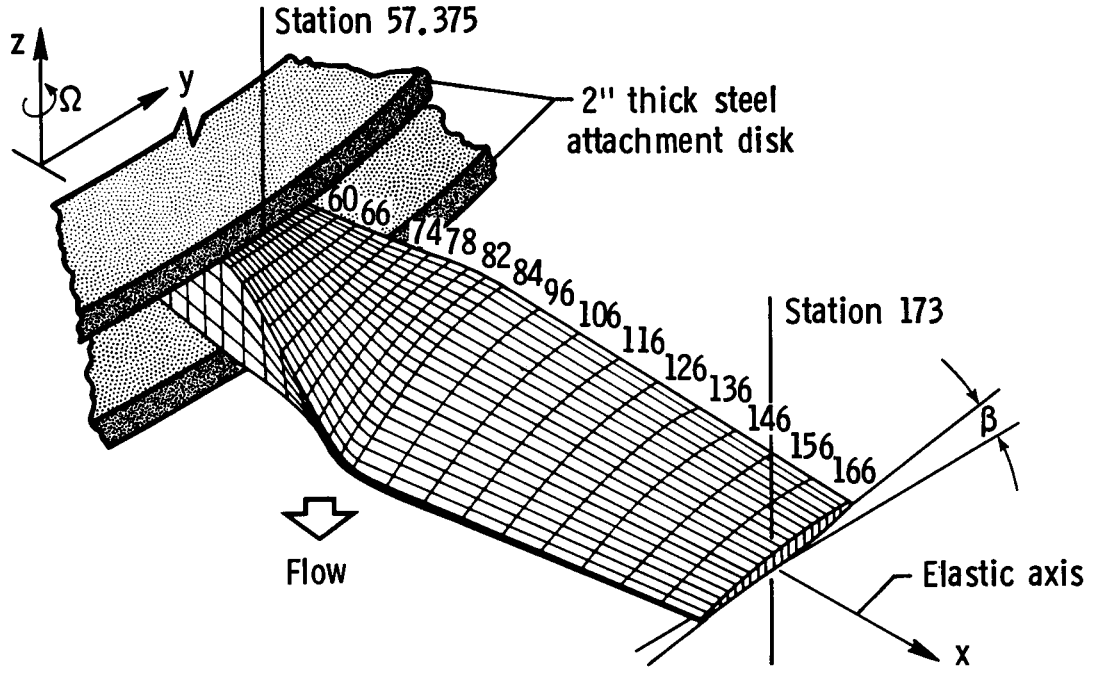

Fig B.2 7- by 10-Foot Wind Tunnel fan blade

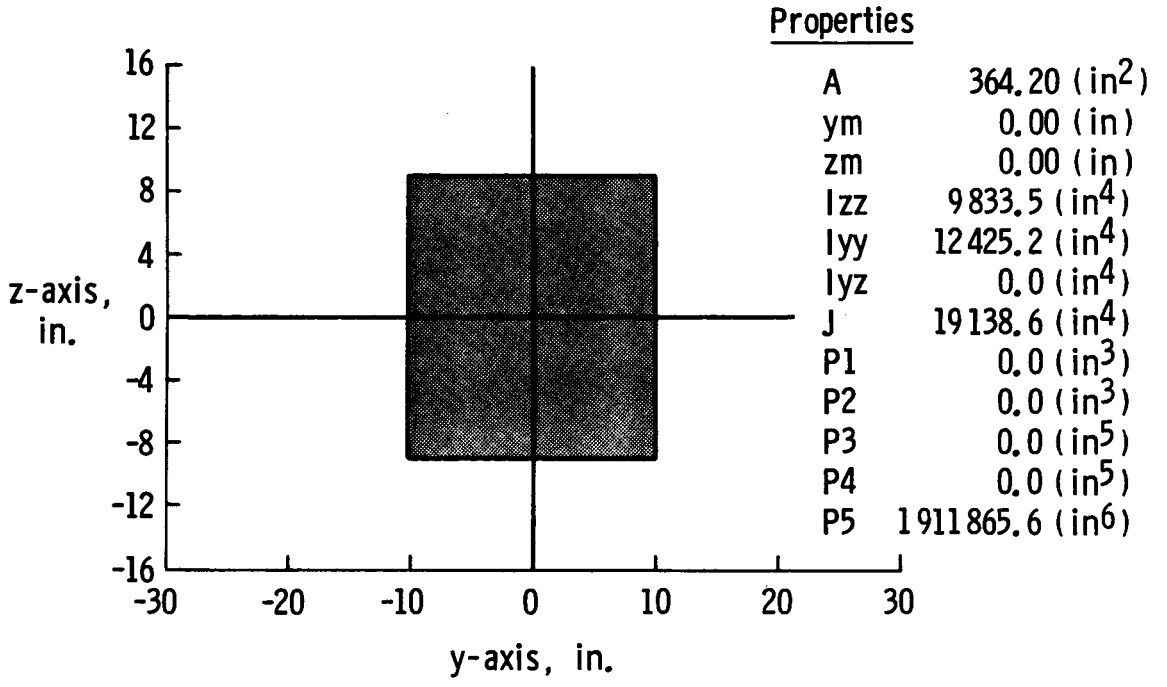

Fig B.3 7- by 10-Foot Wind Tunnel fan blade station 57.375

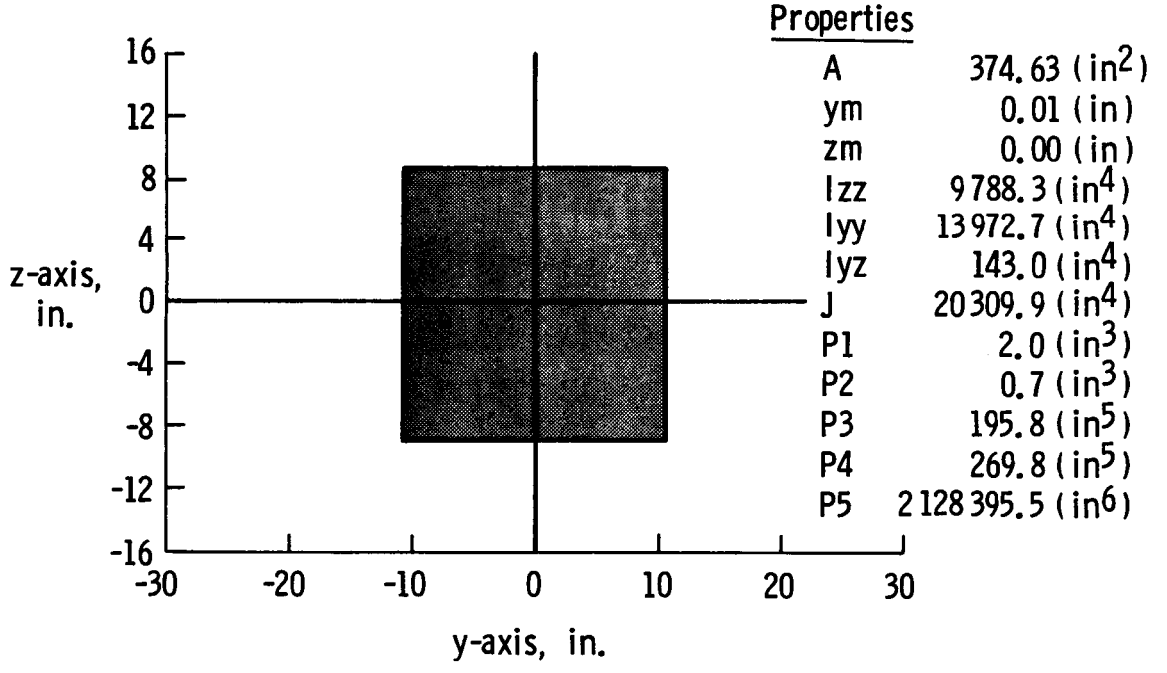

Fig B.4 7- by 10-Foot Wind Tunnel fan blade station 60.000

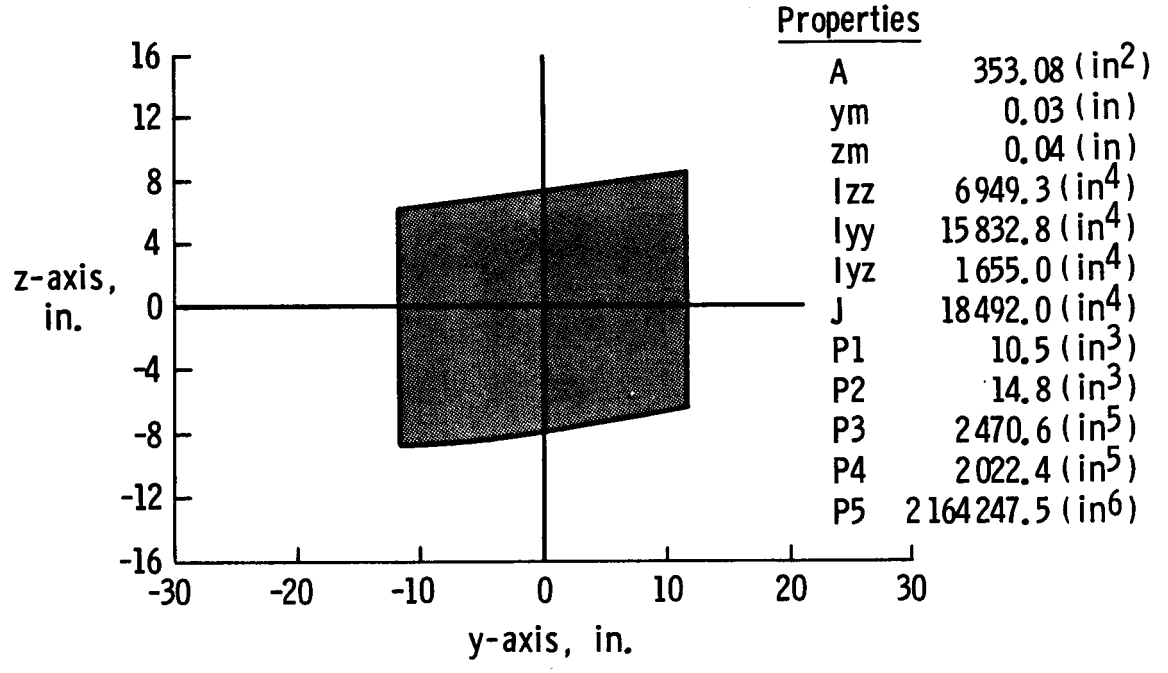

Fig B.5 7- by 10-Foot Wind Tunnel fan blade station 66.000

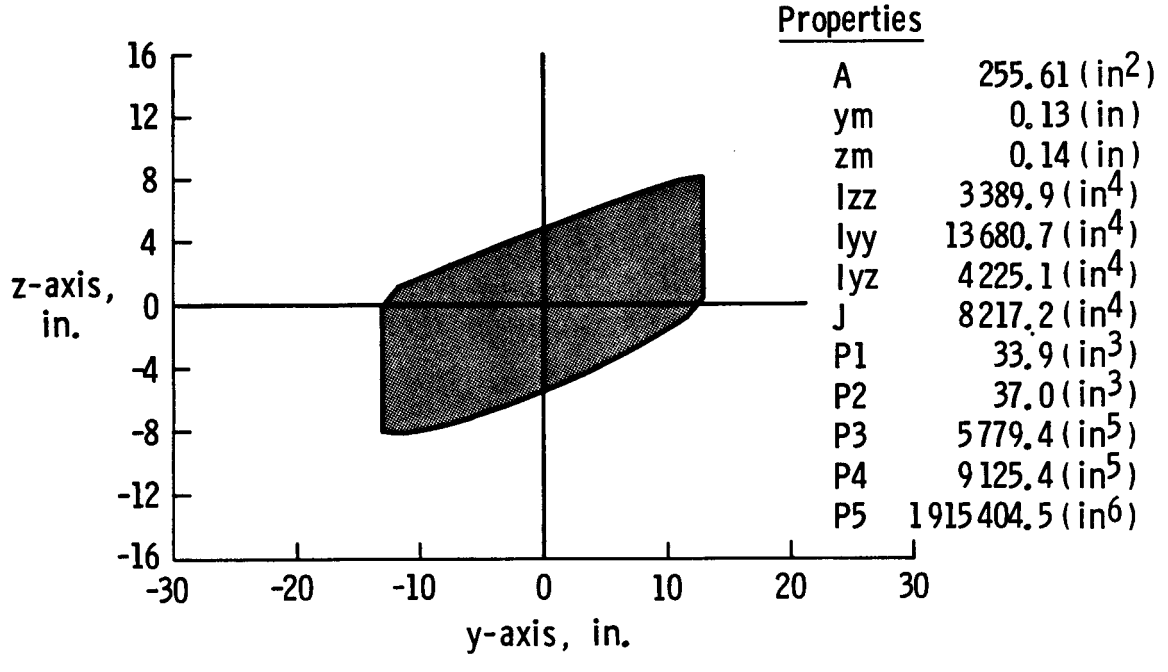

Fig B.6 7- by 10-Foot Wind Tunnel fan blade station 74.000

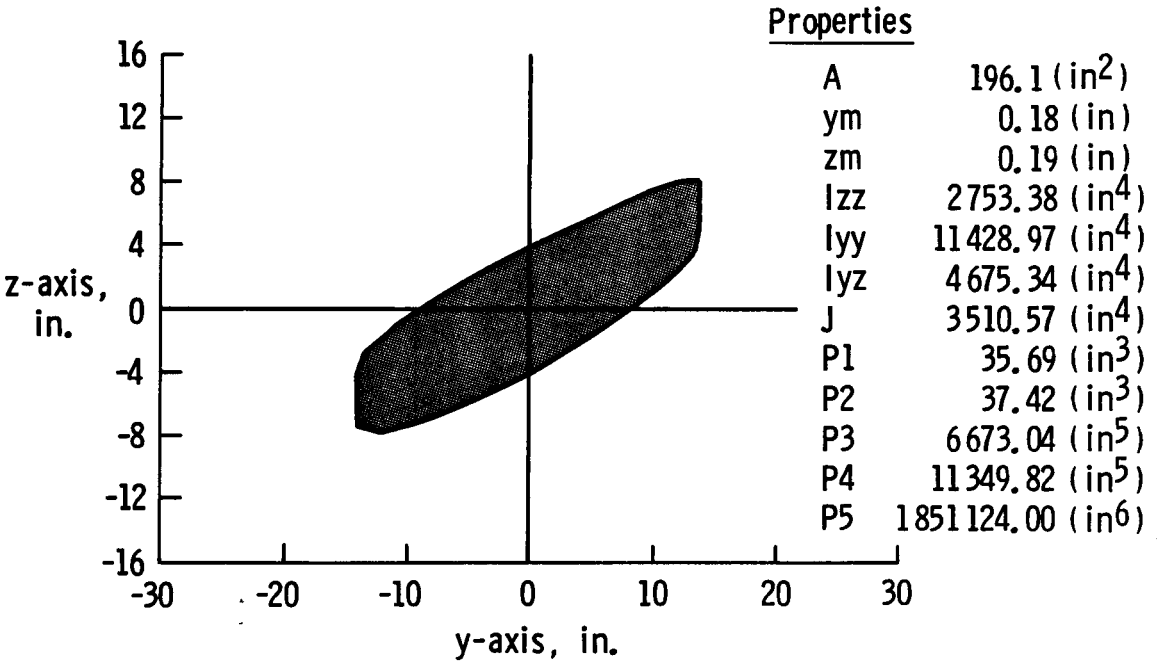

Fig B.7 7- by 10-Foot Wind Tunnel fan blade station 78.000

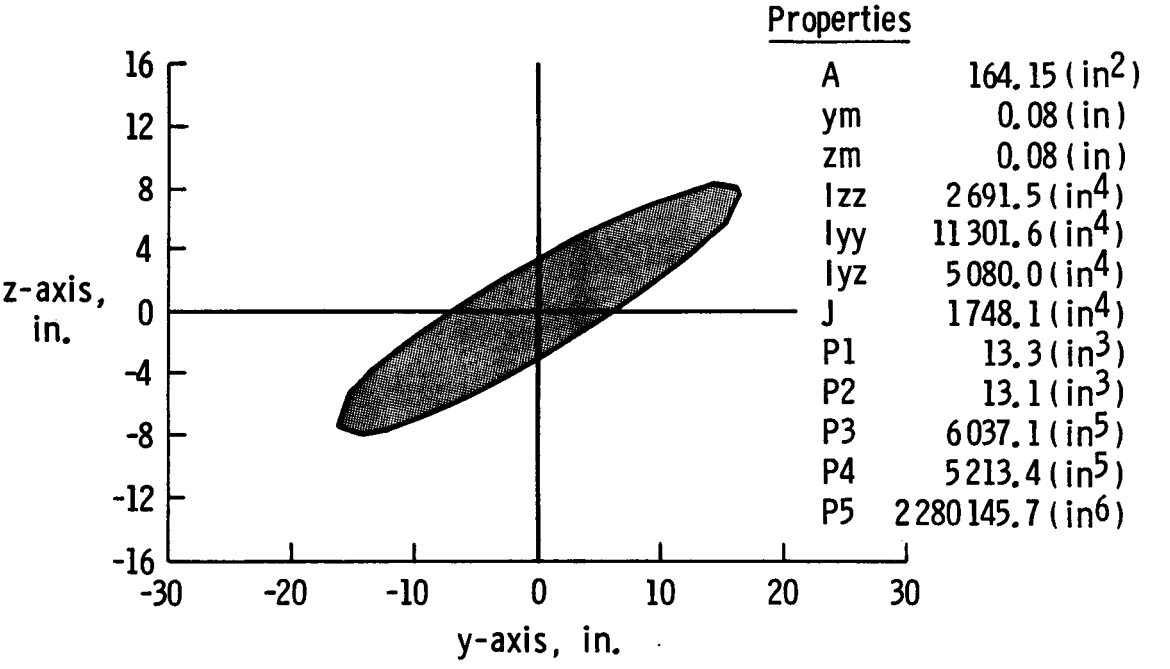

Fig B.8 7- by 10-Foot Wind Tunnel fan blade station 82.000

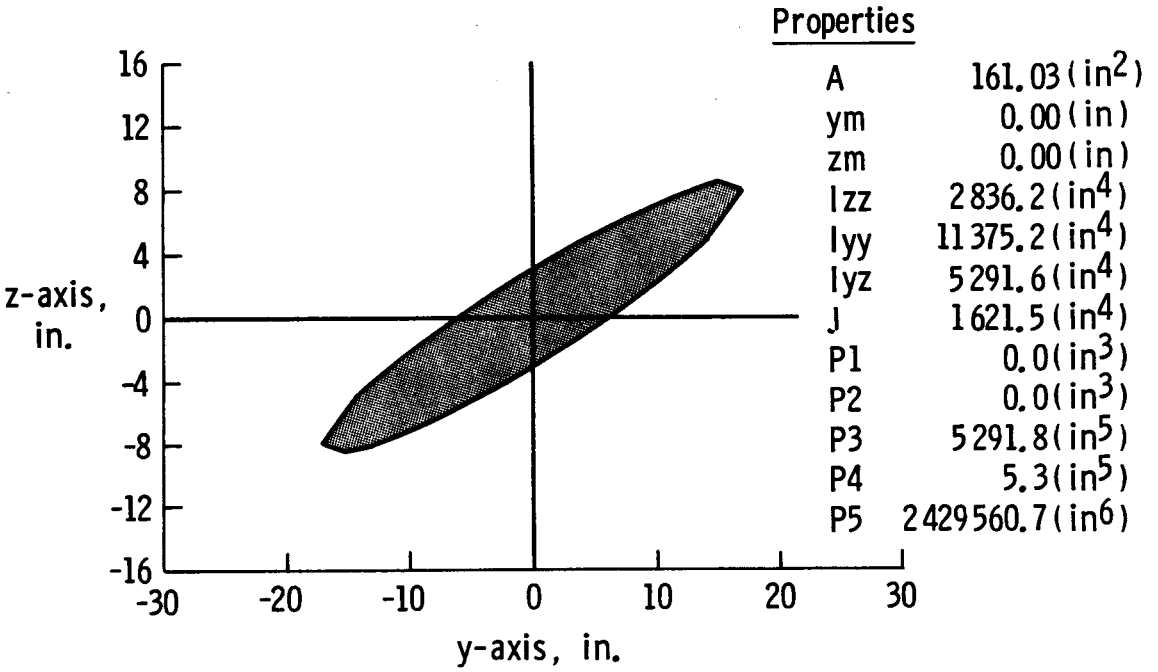

Fig B.9 7- by 10-Foot Wind Tunnel fan blade station 84.000

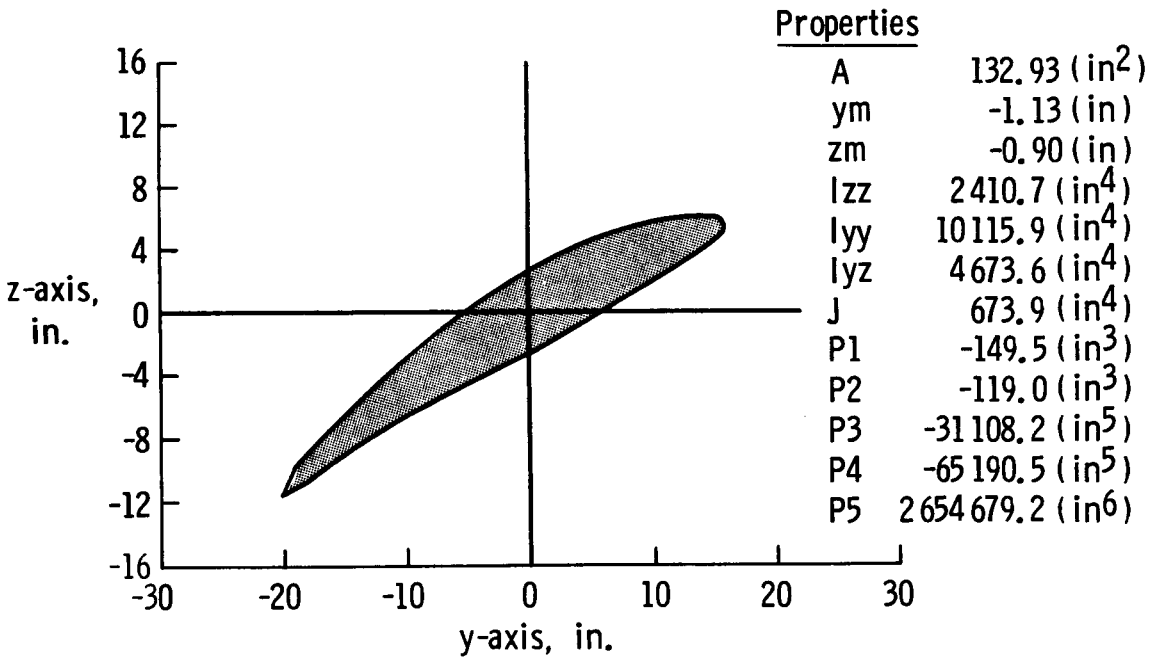

Fig B.10 7- by 10-Foot Wind Tunnel fan blade station 96.000

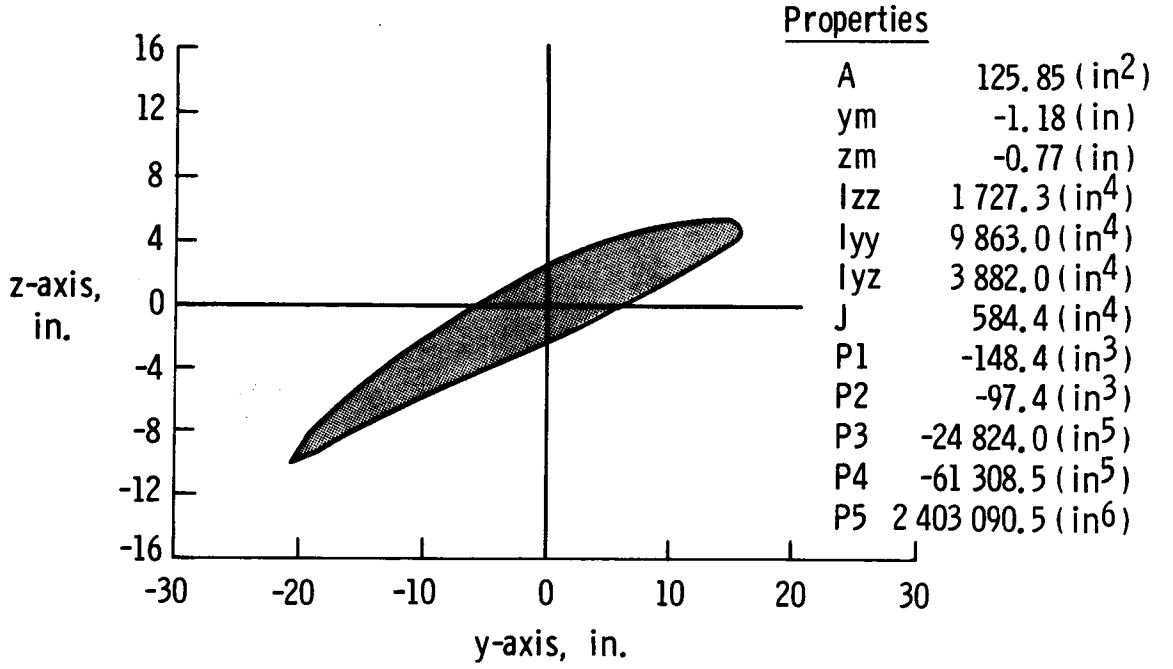

Fig B.11 7- by 10-Foot Wind Tunnel fan blade station 106.000

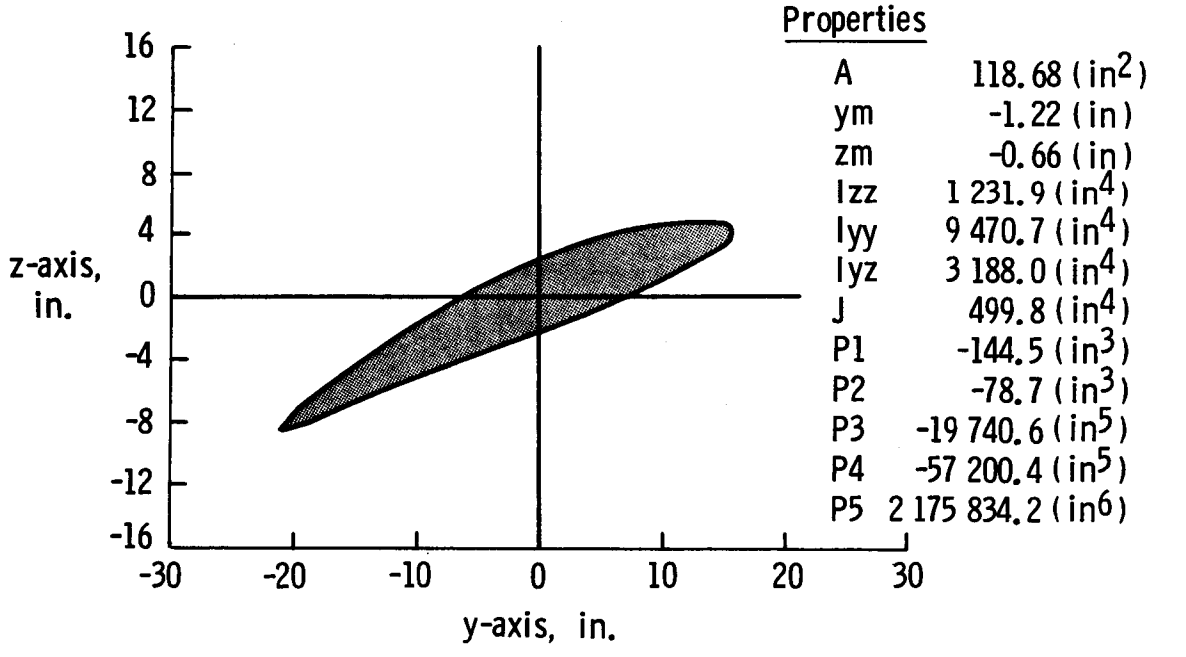

Fig B.12 7- by 10-Foot Wind Tunnel fan blade station 116.000

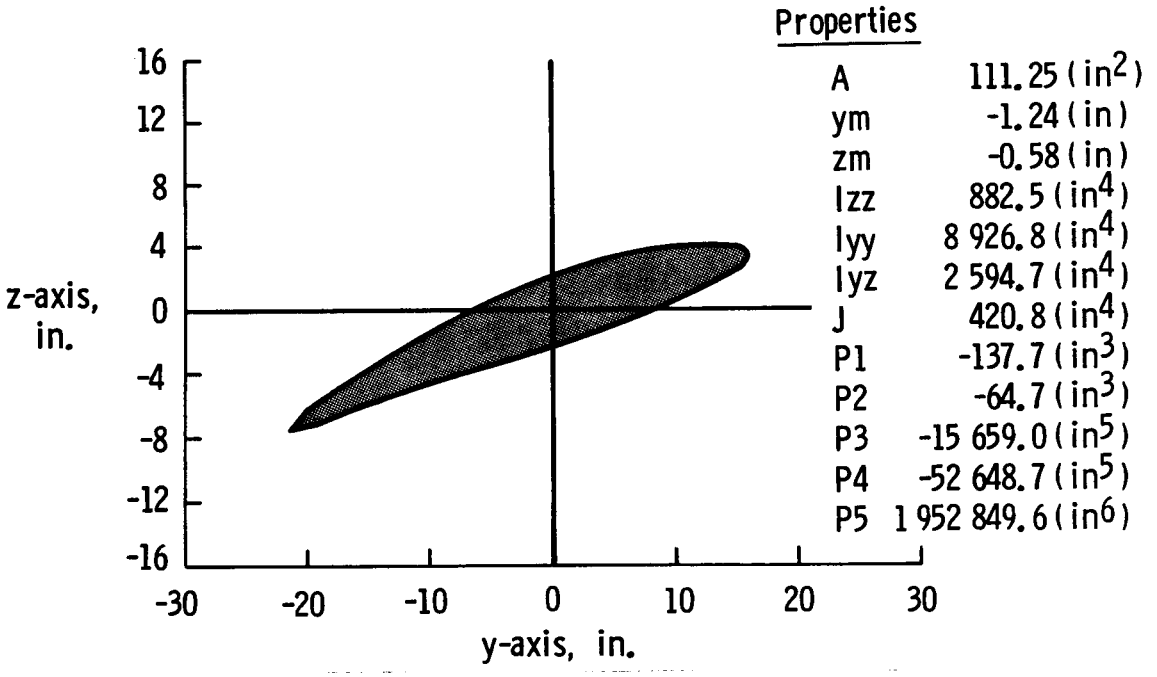

Fig B.13 7- by 10-Foot Wind Tunnel fan blade station 126.000

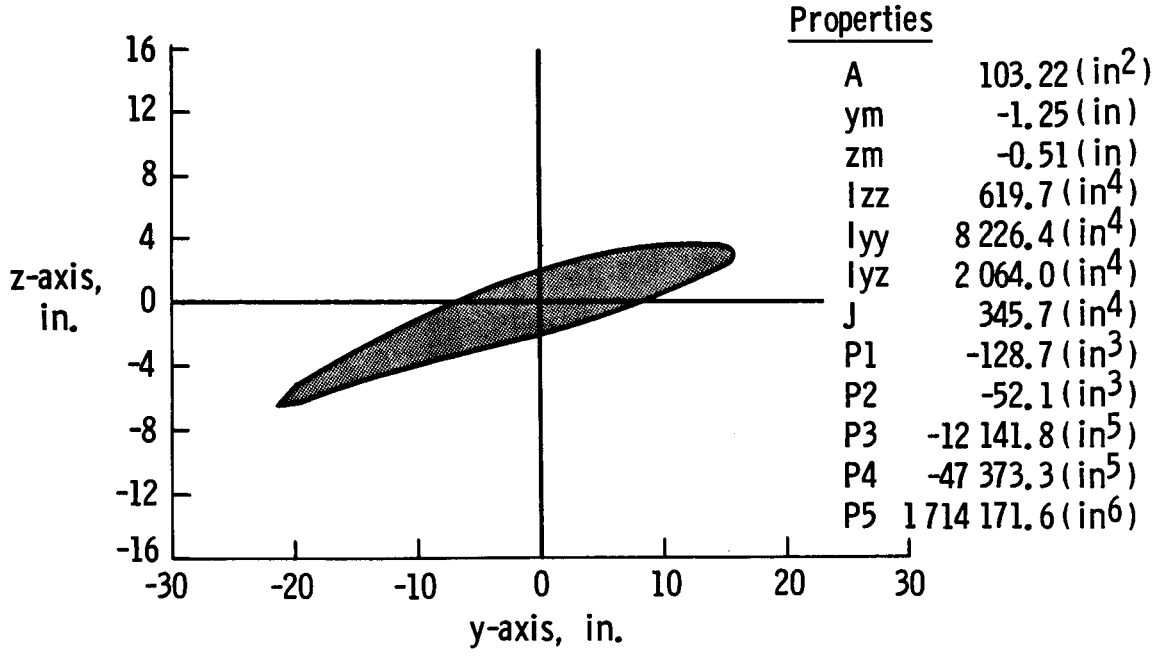

Fig B.14 7- by 10-Foot Wind Tunnel fan blade station 136.000

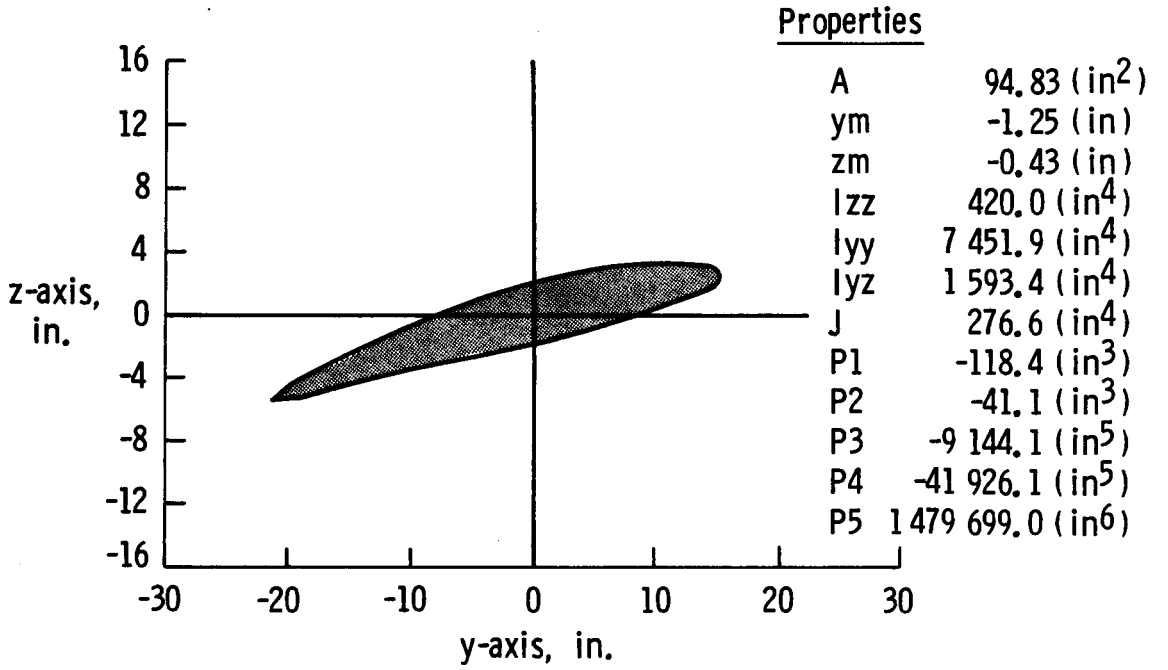

Fig B.15 7- by 10-Foot Wind Tunnel fan blade station 146.000

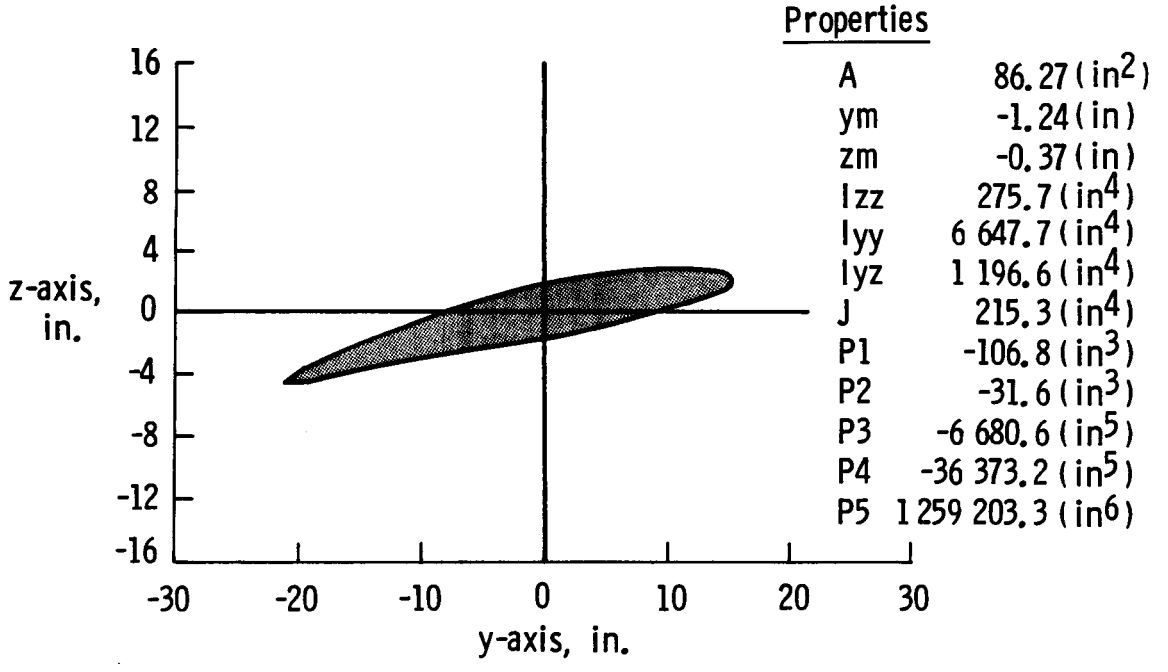

Fig B.16 7- by 10-Foot Wind Tunnel fan blade station 156.000

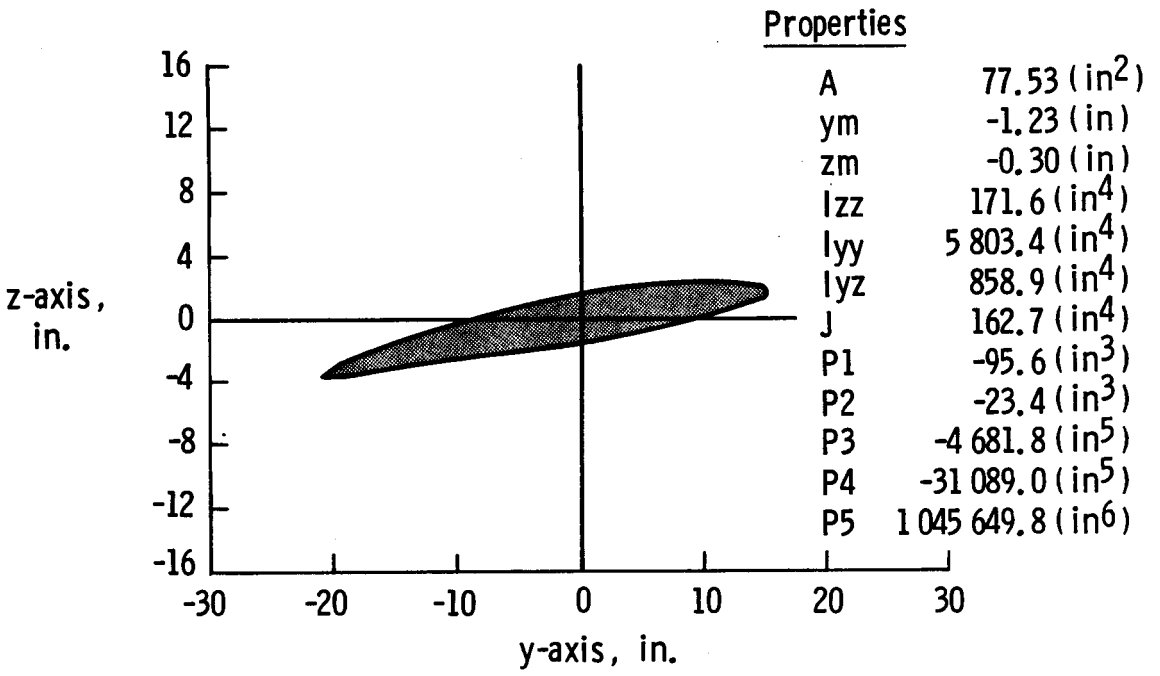

Fig B.17 7- by 10-Foot Wind Tunnel fan blade station 166.000

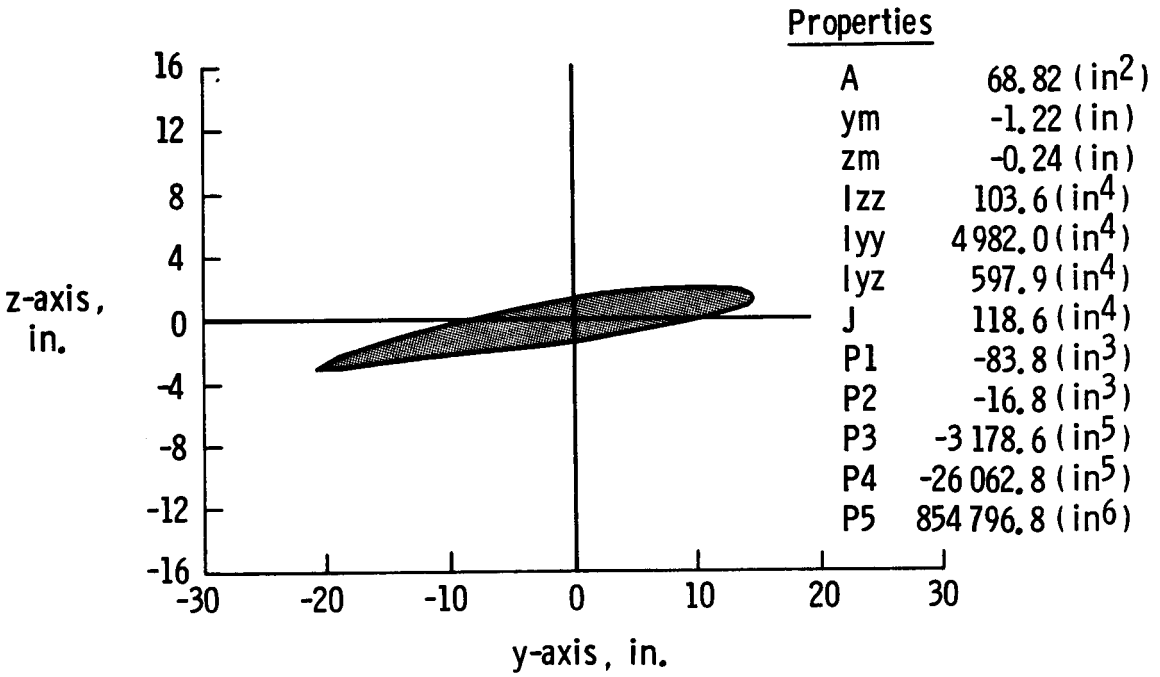

Fig B.18 7- by 10-Foot Wind Tunnel fan blade station 173.000

NASA National Aeronautics and Space Administration

Report Documentation Page

1. Report No.	2. Government Accession No.	3. Recipient's Catalog No.
NASA TM-100596		

4. Title and Subtitle	5. Report Date
Coupled Bending-Torsion Steady-State Response of Pretwisted, Nonuniform Rotating Beams Using a Transfer-Matrix Method	March 1988
	6. Performing Organization Code

7. Author(s)	8. Performing Organization Report No.
Carl E. Gray, Jr.	
	10. Work Unit No.
	505-61-01-07

9. Performing Organization Name and Address	11. Contract or Grant No.
NASA Langley Research Center Hampton, VA 23665-5225	
	13. Type of Report and Period Covered
12. Sponsoring Agency Name and Address	Technical Memorandum
National Aeronautics and Space Administration Washington, DC 20546-0001	14. Sponsoring Agency Code

15. Supplementary Notes

16. Abstract

Using the Newtonian method, the equations of motion are developed for the coupled bending-torsion steady-state response of beams rotating at constant angular velocity in a fixed plane. The resulting equations are valid to first order strain-displacement relationships for a long beam with all other nonlinear terms retained. In addition, the equations are valid for beams with the mass centroidal axis offset (eccentric) from the elastic axis, nonuniform mass and section properties, and variable twist. The solution of these coupled, nonlinear, nonhomogeneous, differential equations is obtained by modifying a Hunter linear second-order transfer-matrix solution procedure to solve the nonlinear differential equations and programing the solution for a desk-top personal computer. The modified transfer-matrix method was verified by comparing the solution for a rotating beam with a geometric, nonlinear, finite-element computer code solution; and for a simple rotating beam problem, the modified method demonstrated a significant advantage over the finite-element solution in accuracy, ease of solution, and actual computer processing time required to effect a solution.

17. Key Words (Suggested by Author(s))	18. Distribution Statement
Fan blades, numerical methods, transfer matrix, rotating beam	Unclassified - Unlimited Subject Category 39

19. Security Classif. (of this report)	20. Security Classif. (of this page)	21. No. of pages	22. Price
Unclassified	Unclassified	98	A05

NASA FORM 1626 OCT 86